# The water and energy balance of Lake Miwasin: a pilot-scale oil sands pit lake

by

Austin Zabel

A thesis

presented to the University of Waterloo

in fulfilment of the

thesis requirement for the degree of

Master of Science

in

Geography (Water)

Waterloo, Ontario, Canada, 2024

## Author's Declaration

This thesis consists of material all of which I authored or co-authored: see Statement of Contributions included in the thesis. This is a true copy of the thesis, including any required final revisions, as accepted by my examiners.

I understand that my thesis may be made electronically available to the public.

## Statement of Contributions

Austin Zabel was the sole author for Chapters 1, 3, and 4 which have not at this time been submitted for publication.

Austin Zabel was the primary author of Chapter 2 which has been published open access through the International Journal of Mining, Reclamation and Environment. Dr. Richard Petrone and Dr. Scott Ketcheson were co-authors on the paper contributing intellectual input.

Citation:
Austin Zabel, Scott J Ketcheson & Richard M Petrone (2024) Climatic controls on the water balance of a pilot-scale oil sands mining pit lake in the Athabasca oil sands region, Canada, International Journal of Mining, Reclamation and Environment, 38:4, 306 323, DOI: 10.1080/17480930.2023.2270301.

## Abstract

Energy companies in the Athabasca Oil Sands Region in Alberta, Canada are studying the viability of incorporating pit lakes into reclamation closure designs to both sequester tailings and re-integrate the mining lease into the broader natural landscape. Lake Miwasin is a pilot-scale oil sands pit lake encompassed by a constructed catchment where the volume of the water cap is not actively managed. This research quantified the water and energy balances of Lake Miwasin during the open water season for two consecutive years. As the constructed catchment lacks both natural waterbodies and connectivity to a legacy groundwater system, freshwater additions to the lake during the summer season were governed by rainfall. Above average rainfall during the first year triggered surface water inflow events that diluted the over-winter water volume by ~ 25%. The second year had below average rainfall resulting in minimal surface water inflow and a 30 cm drop in lake stage. The lake became thermally stratified during the open water season absorbing high amounts of energy in the spring and releasing this energy in late summer/fall. Despite being constructed at a pilot-scale, the timing and magnitude of the maximum heat content were comparable to small natural waterbodies. The small fetch and surrounding landscape features led to a sheltering effect reducing wind action at the surface contributing to lower correlations between climatic variables and the surface energy fluxes compared to larger neighboring lakes. This research indicates variable climatic conditions, lake size, and surrounding landscape features will influence the water balance and energetics of future oil sands pit lakes. Consideration of the presented results and continued research is required to guide the implementation of these contemporary landscape features throughout the Athabasca Oil Sands Region.

## Acknowledgements

I would like to thank Jennifer Attema, Adam Green, and the Field Services team at Suncor Energy for field assistance with this research. I also thank Hatfield Consultants for providing site data and communications. Funding from a research grant awarded to SK and RP from Suncor Energy Inc. is gratefully acknowledged.

I also acknowledge that this research occurred within the boundaries of Treaty 8, traditional lands of the Dene and Cree, as well as the traditional lands of the M´etis of northeastern Alberta.

# Table of Contents

# List of Figures

# List of Tables

## List of Abbreviations and Symbols

| | |
|---|---|
| AOSR | Athabasca Oil Sands Region |
| BML | Base Mine Lake |
| cal | Calorie |
| CEMA | Cumulative Environmental Management Association |
| cm | Centimeter |
| $C_O$ | Concentration of Old Water |
| CSTR | Continuously Stirred Tank Reactor |
| $C_{\rho a}$ | Specific Heat Capacity of Air at Constant Pressure |
| E | Evaporation |
| e | Euler's Number |
| F | Flux |
| FT | Fluid Tailings |
| $f_b$ | Volumetric Fraction of Bitumen |
| $f_S$ | Volumetric Fraction of Solids |
| $f_W$ | Volumetric Fraction of Water |
| g | Grams |
| GW | Groundwater |
| H | Heat Content |
| ha | Hectare |
| $H_{L1}$ | Energy Stored within the Top Layer of the Water Column |
| Hz | Hertz |
| IP | Instrument Pole |
| J | Joules |
| K | Kelvin |
| kg | Kilograms |
| L | Latent Heat of Vaporization |
| m | Meter |
| mm | Millimeter |
| P | Precipitation |
| PASS | Permanent Aquatic Storage System |
| q' | Dry Mol Fraction of Water Vapor |
| $Q_A$ | Net Advected Energy |
| $Q_e$ | Latent Heat |
| $Q_g$ | Lake Sediment Heat Flux |
| $Q_h$ | Sensible Heat |
| $Q_n$ | Net Radiation |

| | |
|---|---|
| Rg | Global Radiation |
| rH | Relative Humidity |
| s | Second |
| S | Specific Heat Capacity of Pure Water |
| s' | Dry Mol Fraction |
| SVP | Saturated Vapor Pressure |
| SW | Surface Water |
| T | Temperature |
| $T_a$ | Air Temperature |
| $T_O$ | Volume of Water Released from Tailings |
| $T_S$ | Temperature of Lake Sediment |
| $T_V$ | Virtual Temperature |
| $T_W$ | Water Temperature |
| U | Horizontal Wind Speed |
| U* | Friction Velocity |
| UPL | Upper Pit Lake |
| $V_I$ | Volume of Surface Water Inflow |
| $V_{Mix}$ | Volume of Water in the Mixed Layer |
| $V_O$ | Old Water |
| $V_{OM}$ | Volume of Old Water in the Mixed Layer |
| VPD | Vapor Pressure Deficit |
| W | Watt |
| w' | Vertical Wind Speed |
| ws | Water-Sediment Interface |
| $\Delta Q_S$ | Change in Energy Storage |
| $\Delta S$ | Change in Storage |
| $\lambda$ | Thermal Conductivity |
| $\lambda_b$ | Thermal Conductivity of Bitumen |
| $\lambda_S$ | Thermal Conductivity of the Solid Particles |
| $\lambda_W$ | Thermal Conductivity of Water |
| $\rho a$ | Air Density |

# Chapter 1 – Introduction

Canadian indigenous peoples utilized the natural oil sands resources in northern Alberta for centuries before written notes by an American explorer in 1778 recounted the existence of a black tar-like substance naturally seeping from the ground (Chastko, 2004). During a geological survey conducted between 1882-1883, observations of natural gas bubbling along the banks of the Athabasca River, visible bands of lignite and petroleum bearing sandstone, and liquid tar oozing out of clear water springs led scientist Robert Bell to assert the petroleum substances in the Athabasca Region be "regarded as of great scientific and economic importance" (Bell, 1884). In 1913, the Canadian Government placed the oil sands on reserve and enabled researcher Sidney Ells to travel to Fort McMurray to collect samples and further examine the region (Chastko, 2004). Following a decade of scientific inquiry, Dr. Karl Clark, working as a scientist for the Scientific and Industrial Research Council of Alberta, and colleagues at the University of Alberta built a hot water separation plant in 1923 and patented a process to extract the bitumen from the oil sands by 1929 (Chastko, 2004; Humphries, 2007). Phase separation of the bitumen was achieved by mixing the mined oil sands with water, sodium hydroxide, and steam within a heated rotating drum (Schramm, 2001). The scalability and practicality of the extraction process was proven over the next 30 years allowing for incorporation into the first commercial oil sands production facility commissioned in 1967 (Humphries, 2007). By 2020, the Alberta Oil Sands were producing 2.84 million barrels of oil a day supporting over 2300 companies across Canada and adding billions of dollars to provincial and federal revenue (CAPP, 2022).

The hot water separation process used in the oil sands enables the extraction of bitumen from the mined matrix but produces a by-product mixture of sand, clay, water, silt, salts, trace metals, residual bitumen, and other hydrocarbons, referred to as tailings (Government of Alberta,

2015; Alberta Energy Regulator, 2020). These tailings contain fine silt and clay particles with unique electrochemical properties that cause them to resist coagulation and remain suspended in a fluid state for several decades prior to settling (Fair, 2014). This fluid matrix, referred to as Fluid Tailings (FT), has continued to accumulate over the past 50 years at a rate far beyond initial expectations with no significant single solution presented to enhance consolidation of the fine particles at a large scale (Fair, 2014; Read, 2014). As of 2019, it was estimated that there are over 1.2 billion cubic meters of FT stored within the Athabasca Oil Sands Region (AOSR) (AER, 2020) posing a substantial environmental liability.

This large repository of FT accumulated as operators were granted rights to mine, work and recover oil sands within areas of land leased from the government (Government of Alberta, 2020) but were prevented from releasing substances that can cause adverse effects to the surrounding environment (Government of Alberta, 2023). In 2012, the Alberta Government developed the Lower Athabasca Regional Plan to implement long term environmental monitoring goals and report on the management of cumulative effects throughout the AOSR (Government of Alberta, 2012). The Tailings Management Framework was then implemented in 2015 with the goals of monitoring and tracking FT accumulation, encouraging progressive treatment of FT during operations, and ensuring FT are ready-to-reclaim within 10 years of the end of mine life (Government of Alberta, 2015). To be classified as ready-to-reclaim, the tailings must be treated with an approved technology, deposited in their permanent location, and meet performance criteria regarding their physical properties and likelihood of compromising the surrounding environment (Alberta Energy Regulator, 2017). Reclaiming FT is a regulatory requirement and part of a larger objective to return leased lands disturbed during oil sands exploration to the crown in a state

representative of the natural boreal ecosystem (Alberta Energy Regulator, 2017; Government of Alberta, 2023).

Water-capping is one technology being assessed for FT reclamation and it involves storing FT beneath a mixture of process affected water and freshwater creating a lake intended to eventually support aquatic life (Alberta Energy Regulator, 2017; Alberta Energy Regulator, 2020). Research into water-capping began in the 1980's as Syncrude Canada Ltd. developed a series of test ponds and demonstrated potential for continued tailings consolidation and the improvement of water quality over time (Read, 2014). After decades of study and a large body of published scientific research, the Alberta government granted Syncrude Canada Ltd. approval to commission the first commercial-scale test lake employing the water-capping technology in a previously mined pit (Read, 2014; Dompierre et al., 2016). In 2012, the West In-Pit tailings disposal area became Base Mine Lake (BML) and remains the only commercial scale oil sands pit lake in the AOSR (Dompierre et al., 2016).

In 2017, Suncor Energy Inc. constructed a second oil sands pit lake to further develop their Permanent Aquatic Storage System (PASS); a process that involves adding a coagulant and flocculant to FT prior to deposition beneath a water-cap (BGC Engineering Inc., 2018). Lake Miwasin was constructed as a pilot-scale project to simulate future commercial applications of the PASS system within Suncor's Millennium Mine lease (BGC Engineering Inc., 2018). Along with storing treated tailings, Lake Miwasin is also unique as it was constructed with an adjacent upland watershed. As the water volume in BML is controlled (Dompierre et al., 2016), Lake Miwasin will provide valuable insight into the sustainability of constructed oil sands pit lakes employing the water-capping tailings treatment technology within the AOSR.

The objective of this thesis is to assess Lake Miwasin's hydrologic and thermal characteristics and their relationship with the design features of the lake basin, the surrounding terrestrial landscape, and the climate of the AOSR. The format of this thesis consists of two manuscripts written as stand-alone documents each addressing a separate portion of the objective. The first manuscript focuses on the water balance and residence time of Lake Miwasin by quantifying the hydrologic fluxes into and out of the lake relative to the change in volume and the limnological conditions throughout the study period. The second manuscript follows a similar approach but quantifies the energy dynamics between the water column, lower atmosphere, and tailings deposit stored within the lake basin. As Lake Miwasin is heavily instrumented, data used in both manuscripts was collected on-site during the open-water season (May – October) of two consecutive years (2020 and 2021). The purpose of these manuscripts is to provide data on the performance of Lake Miwasin for consideration during the planning and design stages of the future commercial scale PASS implementation in Suncor Energy Inc.'s Base Mine lease. Additionally, it is the intention of this thesis to contribute to the existing body of research being utilized to assess the viability of water-capping FT technologies throughout the AOSR in Alberta, Canada.

# Chapter 2 – Climatic Controls on the Water Balance

## 2.1 Introduction

Oil sands mining operators in Alberta, Canada, are developing reclamation technologies to restore the natural ecological capability of disturbed landscapes and sequester mine tailings. One method of addressing both objectives is by constructing pit lakes to fill in large mined-out pits and cap deposited tailings from the surrounding environment with water (Alberta Energy Regulator, 2017). Pit lakes have been regarded as best management practices for mining closure landscapes, with extensive research completed on their incorporation into various resources extraction sites worldwide (Golder Associates, 2017). However, examples of pit lake application in the oil sands context are limited. Base Mine Lake (BML), located within Syncrude's Mildred Lake Mine, was commissioned in 2012 and is the first, and currently only, commercial-scale pit lake in the Athabasca Oil Sands Region (AOSR) (Risacher et al., 2018). Research completed on BML thus far has focused mainly on water quality by looking at naphthenic acids (Bowman et al., 2020; Yu et al., 2019), oxygen availability (Risacher et al., 2018; Arriaga et al., 2019), fluid tailings (FT) geochemistry (Dompierre et al., 2016), turbidity (Tedford et al., 2019; Poon et al., 2018), and toxicity (White and Liber, 2020) of the water cap. However, water quantity is also an important issue as variations in evaporation rates have been reported at BML (Clark et al., 2021; Chang, 2020) and some concern has been raised about the ability of deposited tailings to seal the bottom of pit lake basins in general (Kabwe et al., 2019). As such, evaporative losses from the lakes and the ability of the surrounding watershed to supply sufficient water to maintain stable lake levels are significant design considerations (Dompierre et al., 2016), especially considering climate change. The Cumulative Environmental Management Association (CEMA) has stated the importance of establishing hydrologic connectivity between oil sands pit lakes and their

surrounding reclamation landscapes to manage water flow, maintain adequate water quality, and promote sustainable aquatic ecosystem function (Castendyk et al., 2012). Thus, with over 30 pit lakes planned throughout the AOSR (Burkus et al., 2014), further research is needed to guide the integration of these contemporary waterbodies into both reclamation closure designs and the natural landscape.

AOSR is located within the Boreal Plains ecozone, in a sub-humid climate and composed of hydrologically connected forests, wetlands, ponds, and lakes that respond to variations in both annual and decadal water cycles (Devito et al., 2012). The surficial geology is dominated by fine-grained and coarse-grained glacial till, resulting in both aquitards and aquifers that affect local groundwater availability (Fenton et al., 1994). Water balances for boreal lakes are heavily controlled by both climatic conditions and the surrounding landscape morphology, with large variations occurring between individual lakes (Gibson et al., 2002; Bennett et al., 2008) and inter-annually within the same lakes (Schmidt et al., 2010). Annually, most precipitation (~70%) and evaporation occur between May and September (Devito et al., 2012), making summer climatic conditions particularly important for boreal lake hydrology. During summer precipitation events, surface and groundwater inflows and outflows are heavily influenced by local soil texture (Ferone and Devito, 2004; Smerdon et al., 2005). Runoff ratios and surface water yields to boreal lakes are also highly variable and influenced by catchment characteristics such as topography, size, vegetation cover, surficial geology, the existence of permafrost, and the presence of hydrologic features such as bogs, fens, open-water wetlands, and streams (Gibson et al., 2015; Devito et al., 2017). Evaporation plays a significant role in water loss from northern lakes (Gibson, 2002) with rates influenced by surrounding landscape features and meteorological conditions (Petrone et al., 2007). As future changes in climate are expected to impact water availability throughout the Boreal

Plains (Ireson et al., 2015), understanding hydrologic connections between boreal lakes, their surrounding landscapes and catchments, and local climatic conditions will be essential for the management of both natural and constructed pit lakes.

Wetzel (2001) describes the importance of catchments and basin dimensions to the development and existence of natural lakes. Constructed waterbodies often have atypical basin dimensions and exist within altered catchments resulting in either controlled or highly variable hydrologic conditions. For example, reservoirs have high catchment to surface area ratios, high stream order tributaries, large and irregular volume fluctuations, and controlled outflows (Wetzel, 2001). Stormwater ponds are often designed with low volume to surface area ratios, and lined basins to prevent seepage (Eger et al., 2014), and can experience surface inflow events from piped systems that introduce over 100% of the pond volume in less than 24 hours (Walker, 1998). Pit lakes are formed in a variety of excavations created during resource extraction and can vary substantially compared to natural lakes in terms of surface area to depth ratios (Gammons et al., 2009; Golder Associates, 2017). Typically, pits infill with groundwater, precipitation, run-off, or actively pumped water once mining activities cease (Castro and Moore, 2000). In arid or sub-humid climates, evaporation rates can exceed inputs keeping the water level in the pit lower than the surrounding water table forming a terminal lake (McCullough et al., 2013). Terminal pit lakes are susceptible to poor water quality and acidification over time from oxidation of minerals in the surrounding rock, collection of solutes via groundwater input, and evapoconcentration (Eary, 1998). These processes can create surface water quality that is toxic to the surrounding environment and lead to density-driven releases from the pit to the surrounding groundwater if sufficient concentrations of solutes are reached (Mccullough et al., 2012a). Flow-through pit lakes allow directional water flow through the pit and are common at mine sites where there is a natural

slope in the groundwater table, in wet climates with high water inputs, or when the pit receives regular surface water inflow (Gammons et al., 2009). Flow-through conditions can also be initiated by diverting existing streams into a pit (Brinker et al., 2011; McCullough et al., 2012b; McCullough and Schultze, 2018). The inflow of freshwater can improve pit lake water quality by diluting concentrated solutes, neutralizing acidity, and introducing aquatic organisms (McCullough and Schultze, 2018) that can help establish biotic communities and promote higher end uses such as fisheries (Brinker et al., 2011). Lund et al. (2020) demonstrate the benefit of reclaiming catchments even in the absence of a connecting watercourse, as runoff can still transport valuable nutrients into a pit lake. However, this method offers far less consistent inputs as runoff depends on precipitation, and the hydrology of reclaimed hillslopes has been observed to change over time (Ketcheson and Price, 2016).

The movement of water within and through a lake can dictate the accumulation of dissolved and suspended substances impacting the biological and chemical characteristics of the system (Monsen et al., 2002; Ambrosetti et al., 2003). Lake hydrology and limnology, therefore, effect water quality and can be conceived with measures of water-mass retention such as residence time and flushing time (Monsen et al., 2002). These are often estimated using the idealized conditions of a continuously stirred tank reactor (CSTR) where there is complete vertical and horizontal mixing, and steady-state inflow and outflow (Levenspiel, 1998). Other methods applied to transit time estimations are completed using tracers (Cole and Pace, 1998), stable water isotopes (Petermann et al., 2018), and hydrodynamic models (Spigel and Imberger, 1980; Rueda and Cowen, 2005). However, their applications can be limited due to their technical difficulty, cost, and high computational demand.

Pilotti et al, (2014a) applied a simple model (referred to as Tonolli's model) to estimate the flushing time of a stratified lake by assuming complete mixing in the horizontal direction but limiting the vertical mixing based on the presence of a thermocline. The thermocline is a layer where water temperature changes rapidly with depth causing a distinct change in density that can act as a physical barrier and limit the transport of water and nutrients across its plane (Fiedler, 2010). The depth of the thermocline in the water column changes throughout the year and can be used to identify the depth of the surface mixing layer (Fiedler, 2010). Pilotti et al, (2014a) applied temperature data and water budget theory to estimate the flushing time of stratified lakes by applying the CSTR concept to the mixed layer above the thermocline and assuming mixing across the thermocline to be negligible. The application of Tonolli's model is restricted to periods of stratification and is not applicable when surface water inflow is denser than the water in the mixed layer (Pilotti et al., 2014a). Despite the assumptions and restrictions, this model offers an approach to assessing the impacts of surface inflow on the flushing and residence time of a stratified lake (Pilotti et al., 2014a).

To understand the role of hydrology in pit lake function and sustainability, the factors that lead to the largest variations in hydrological processes must be identified (Devito et al., 2005). This study will compare the water balance of a pilot oil sands pit lake during the open water season (May-October) over two consecutive years with varying levels of summer precipitation. Residence time theory will be applied to infer lake mixing and exchange characteristics with the constructed upland watershed. The objective of this research is to identify how variations in summertime precipitation will affect the water balance and residence time of an oil sands pit lake encompassed within a constructed landscape.

## 2.2 Materials and Methods

### *2.2.1 Site Description*

Lake Miwasin is a pilot-scale oil sands pit lake constructed near Suncor's Millennium Mine and is a scaled-down version of the planned Upper Pit Lake (UPL), located in the current Dedicated Disposal Area 3 (BGC Engineering Inc., 2018a). In 2017, roughly 40,000 $m^3$ of treated tailings were deposited into the 12 m deep pit, with the base sitting 10 meters above the Wood Creek Sand Channel aquifer (BGC Engineering Inc., 2018b). By May of 2020, the tailings had settled to a height of ~5.5 meters under a 4.5 m thick water cap with a maximum fetch of 165 m and a surface area of ~12,000 $m^2$ developed on top of the tailings. The lake receives surface water inflow through a single channelized inlet connecting the lake to a constructed upland. The uplands (~9 hectares) are composed of hummocks, swales and developing vegetation, and are located to the east of the lake. The west side of the lake sits ~20 m from a forested edge with an average tree height of 8.5 m. A littoral zone was constructed along the east side of the lake with an area of ~2,600 $m^2$ and a 4% slope. The lake inlet is situated within the littoral zone and is built up ~1 m above the expected lake water level. Surface water from the uplands flows through a 3" Parshall flume installed on a v-notch weir plate and down a section of cobblestone into the lake. The lake outlet is a steel corrugated pipe penetrating through the pit wall near the lake's northwest corner and sits ~10.5 m above the pit base. The top of the pit walls are built up ~1 m from the surrounding ground level creating a berm on the north, west, and south sides preventing overland runoff into the lake from areas other than the constructed upland. The top 5.5 m of the pit walls are also lined with a 60 cm thick compacted clay layer which is expected to minimize exchange between the Lake Miwasin water cap and the surrounding groundwater system (BGC Engineering Inc., 2018b).


**Figure 1:** Lake Miwasin and adjacent uplands are located roughly 20 km north of Fort McMurray AB, Canada within Suncor Energy Inc. millennium mine lease.

### *2.2.2 Instrumentation and Data Collection*

Five instrument poles (IP 01 – 05) were installed in the middle of the lake to house instruments for monitoring the deposited tailings and water cap. The lake surface elevation is tracked by a SR50A sonic ranging sensor (Campbell Scientific Ltd., Utah, USA). A PSA-916 sonar altimeter (Teledyne Benthos, MA, USA) measures the distance from the lake surface to the tailings interface (mudline) delineating the water cap depth. The depth was corrected for variable speeds of sound with daily averaged water temperature (Hatfield, 2022). Temperature thermistors were installed on IP 1-5 at depths of 0.75 m, 1.50 m, 2.25 m, 3.00 m, 3.75 m, and 4.00 m. Values were collected every 15 minutes and averaged horizontally across available sensors to ascertain a thermal profile. EXO2 multiparameter sondes (YSI Inc., Ohio, USA) measured salinity at depths of 2.25 m and 3.75 m. Salinity and temperature were used to calculate water density using the *oce* package in R (R Core Team, 2021). Inflow at the inlet is measured with a 3” Parshall flume (Open Channel Flow, Idaho, USA) instrumented with a Steven’s Smart pressure transducer (Stevens Water

Monitoring Systems Inc., Oregon, USA). A Starflow 6527A ultrasonic doppler flow sensor (Unidata Pty Ltd., WA, Australia) is installed at the downstream end of the outlet culvert to record surface water outflow. Rainfall is collected using a TE525M tipping bucket rain gauge (Campbell Scientific Ltd., Utah, USA) located at the meteorological station on the north side of the lake. The dock beside the inlet has an open-path IRGASON Eddy Covariance system (Campbell Scientific Ltd., Utah, USA) sampling flux values at 20 Hz and calculating averages every 30-minutes on a CR1000x data logger (Campbell Scientific Ltd., Utah, USA). There is also a network of soil moisture and water potential sensors (Decagon Devices Inc., WA, USA), vibrating wire piezometers (RST Instruments Ltd., BC, Canada) and groundwater monitoring wells (Rice Engineering and Operating Ltd., AB, Canada) surrounding the lake basin to monitor seepage and groundwater levels.

### *2.2.3 Eddy Covariance*

The IRGASON was stationed on the dock beside the inlet with the sensors extended over the lake surface at a height of approximately 1 m. Raw fluxes were sampled at a frequency of 10 Hz, averaged over a half-hour, and the half-hour averages were saved on a CR1000x datalogger (Campbell Scientific, Logan, Utah, USA). All fluxes were corrected for density, sensor separation, time lag and coordinate rotation (double coordinate rotation was used) following common Fluxnet protocols (Webb et al., 1980; Kaimal and Finnigan, 1994; Foken and Leclerc, 2004; Aubinet et al., 2012). The resulting half-hour fluxes were then processed in a custom R-Software script, which filtered each half-hour to ensure that it had at least 80% of the high-frequency records and that there was no potential for dew formation on the IRGA lenses by either precipitation or by comparing the dew point temperature to air temperature (Ta). Additional filtering removed values that were greater than ±3 standard deviations of a moving

average, which consisted of 10 half-hour neighboring values; further filtering was completed to check for physically improbable values. The Kljun et al, (2015) footprint analysis was used to constrain the measured fluxes to be within 80% of the desired site boundaries, using their FFP R-functions. Thereafter, fluxes with a corresponding friction velocity (u*) < 0.10 m $s^{-1}$ were removed from the dataset. The filtered energy fluxes were gap-filled using the MDS method outlined in Reichstein et al. (2005) where Global Radiation (Rg), Vapor Pressure Deficit (VPD), and Ta were used as the gap-filling conditions.

## 2.3 Theory and Calculations

### *2.3.1 Application of Standard Water Balance*

A water balance (or water budget) is a method of assessing the hydrologic characteristics of a system by relating the inputs, outputs, and changes in storage using the following standard formula (Healy et al., 2007),

$$\Delta S = P + GW_{(In)} + SW_{(In)} + T_{(D)} - E - GW_{(Out)} - SW_{(Out)} \quad (1)$$

where terms represent volumes ($m^3$) and $\Delta S$ is the change in storage volume of the water cap, P is the addition from direct precipitation, E is the loss from evaporation, $GW_{(In)}$ is groundwater input, $GW_{(Out)}$ is groundwater loss or seepage from the basin, $SW_{(In)}$ is surface water inflow, $SW_{(Out)}$ is surface water outflow, and $T_{(D)}$ is the volume of water released from the tailings consolidation and dewatering. At Lake Miwasin, the combination of the 60 cm compacted clay liner and consolidating tailings are predicted to sufficiently seal the basin resulting in negligible seepage ($GW_{(Out)}$) (BGC Engineering Inc., 2018b). Further, groundwater elevations within the Wood Creek Sand Channel Aquifer are ~10 m below the bottom of the Lake Miwasin basin resulting in $GW_{(In)}$ also being considered negligible. The presence of a near-surface saturated zone has been observed

in the constructed upland (unpublished data); however, shallow subsurface flow paths present within the upland likely discharge into the surficial channel upstream of the lake inlet and, as such, are included within the $SW_{(In)}$ term of the water budget. Complications with the flow sensor at the outlet have resulted in insufficient data for outflow measurements, thus Eq.1 was rearranged to calculate $SW_{(Out)}$ as a residual term,

$$SW_{(Out)} = P + SW_{(In)} + T_{(D)} - E - \Delta S \quad (2)$$

where volumes of P and E were calculated by multiplying the measured values (mm) by the average lake surface area ($m^2$) for the corresponding year. Lake surface area was measured using the polygon area calculator in Google Earth Pro on dates corresponding with the annual average lake surface elevation. The volume of the Lake Miwasin water cap was calculated using capacity curves (Figure 2). Curve 1 was used to calculate the volume of the basin for any elevation below the littoral zone, while curve 2 was used to calculate the volume of the basin including the littoral zone. The volume of the water cap was calculated as the volume between the water surface and mudline. $\Delta S$ was calculated using the difference in lake level and mudline elevation from the start and end of each study period.

### *2.3.2 Residence Time Calculations*

Residence time is widely applied in studies of hydrologic systems; however, multiple definitions exist for this parameter in the literature. Theoretical residence times for lakes are often computed by dividing the volume of the lake by long-term average outflows, quantifying how long a lake will take to drain if inputs cease (Quinn, 1992). Monsen et al, (2002) provide a similar definition for flushing time using volumetric flow-through instead of outflow and define residence time as the average time a parcel or particle will take to exit from an arbitrary position within the system. By assuming complete mixing between inflowing water and the reservoir in a CSTR, all particles

have the same probability of being removed at a given time and complete removal of the initial constituents only occurs after an infinite time step (Quinn, 1992; Monsen et al., 2002; Pilotti et al., 2014b). Therefore, the average age of a particle and the average residence time in a CSTR is equal to the time required to flush a volume equal to the initial reservoir from the system (Pilotti et al., 2014a; Pilotti et al., 2014b).

#### *2.3.2.1 Application of Tonollis Model*

The application of Tonolli's model requires an understanding of the lake volume-depth curve, a time series of surface inflow events with corresponding temperatures, and a time series of the thermal profile (Pilotti et al., 2014a; Pilotti et al., 2014b). The model operates under three fundamental assumptions: (1) lake volume stays constant during the simulation so inflow and outflow volumes are equal; (2) inflowing water mixes only with the surface mixed layer above the seasonal thermocline; and (3) water flowing out of the lake comes only from the surface mixed layer above the seasonal thermocline (Pilotti et al., 2014a; Pilotti et al., 2014b). Piontelli and Tonolli (1964) applied this model to the large (212 $km^2$) and deep (370 m) Lake Maggiore, which is categorized as oligomictic with full mixing of the water column occurring only once over the 5-year study period (Pilotti et al., 2014a). Piontelli and Tonolli (1964) identified 6 periods throughout each year based on the depth of the seasonal thermocline and used the inflow and outflow during these periods to estimate the volume of original water (referred to as old water $V_o$) remaining in the mixed layer after each period (Pilotti et al., 2014b). Residence time was stated as the time required to dilute the concentration of $V_o$ by 63%, which is equal to the time required to flush the initial volume of the reservoir under CSTR conditions (Quinn, 1992; Monsen et al., 2002; Pilotti et al., 2014b).

At Lake Miwasin, lake volume can be calculated above or below any depth by using the capacity curves (Figure 2). If no thermocline develops, the entire lake is assumed to actively mix, and the volume of the mixed layer ($V_{mix}$) is equal to the volume of the entire lake. If a seasonal thermocline exists, $V_{mix}$ is equal to the volume above the thermocline. At the beginning of the season, all the water in the lake is considered $V_o$. To estimate the residence time, the objective was to calculate how diluted $V_o$ became over the open water season. During each inflow event, the volume of water introduced to the lake ($V_I$) was calculated and assumed to be equal to the volume of outflow. The total volume of the mixed layer before the start of each event was also calculated and expressed as $V_{mix.}$ If the volume of $V_o$ in the mixed layer before the event is known ($V_{OM}$), and the volume of water introduced during the event is known, the fraction of $V_{OM}$ remaining in the mixed layer after the event ($C_o$) can be calculated using,

$$C_o = \frac{V_{OM}}{V_{mix} + V_I} \quad (3)$$

At the start of the season $V_{OM}$ and $V_{mix}$ are equal. After the first inflow event, $C_o$ is multiplied by $V_{OM}$ to provide the volume of old water remaining in the mixed layer. This new volume of $V_{OM}$ is then carried forward and the procedure is repeated for each sequential inflow event. By updating both $V_{mix}$ and $V_{OM}$ as the thermocline deepens, a mass balance of $V_O$ is completed over the open water season. Refer to Pilotti et al. (2014b) for further description of the mathematical formulations.

*2.3.2.2 Delineation of the Seasonal Thermocline*

Lakes in temperate regions exhibit thermal stratification during the summer months as incoming solar radiation increases lake surface temperature, creating a layer of decreased density referred to as the surface mixing layer or the epilimnion (Wetzel, 2001). This layer is turbulent as the water is mixed by kinetic energy introduced from wind stress, convection, and inflows (Imboden and

Wuest, 1995) and is expected to be relatively homogeneous in temperature and density during periods of active mixing (Read et al., 2011). The depth of this layer is a product of lake stability, which refers to the resistance to mixing caused by stratification (Wetzel, 2001). Relative thermal resistance to mixing refers to stability induced by density gradients resulting from changes in temperature and is highest at the seasonal thermocline (Vallentyne, 1957). The thermocline is located below the epilimnion within a larger region of temperature discontinuity called the metalimnion, which acts as a physical barrier to mixing (Wetzel, 2001). For this reason, the location of the seasonal thermocline has been used to delineate the lower extent of the surface mixing layer (Davies-Colley, 1988; Pilotti et al., 2014a; Pilotti et al., 2014b).

The thermocline is defined here as the maximum rate of temperature decrease per depth interval, with a general minimum constraint of 1 °C $m^{-1}$ (Wetzel, 2001). The thermocline was calculated by using the thermo.depth function in the 'rLakeAnalyzer' package (R Core Team, 2021), which implements the split and merge algorithm (Thomson and Fine, 2003). The function was set to identify the deepest thermal step in the profile, assumed to represent the seasonal thermocline, with a minimum density gradient of 0.25 $kg/m^3/m$. This minimum value was selected to represent the high-end density gradients per 1 °C change seen at Lake Miwasin during the warmest summer temperatures (Vallentyne, 1957).

As the intention here was to determine what portion of the Lake Miwasin water cap is mixing with the inflowing surface water, temperature profiles were graphed along with the thermocline depth 24 hours before, during, and 24 hours after each inflow event. As parcels of inflowing water will intrude into a lake until met with water of equal or greater density (Fischer et al., 1979), the inflowing water was only assumed to be entrained in the surface mixing layer if the average temperature of the inflow was warmer than the thermocline. For this analysis, temperature was

used as the sole density indicator and hydrodynamic tracer as the installed temperature thermistors offered the most complete vertical profile.

## 2.4 Results

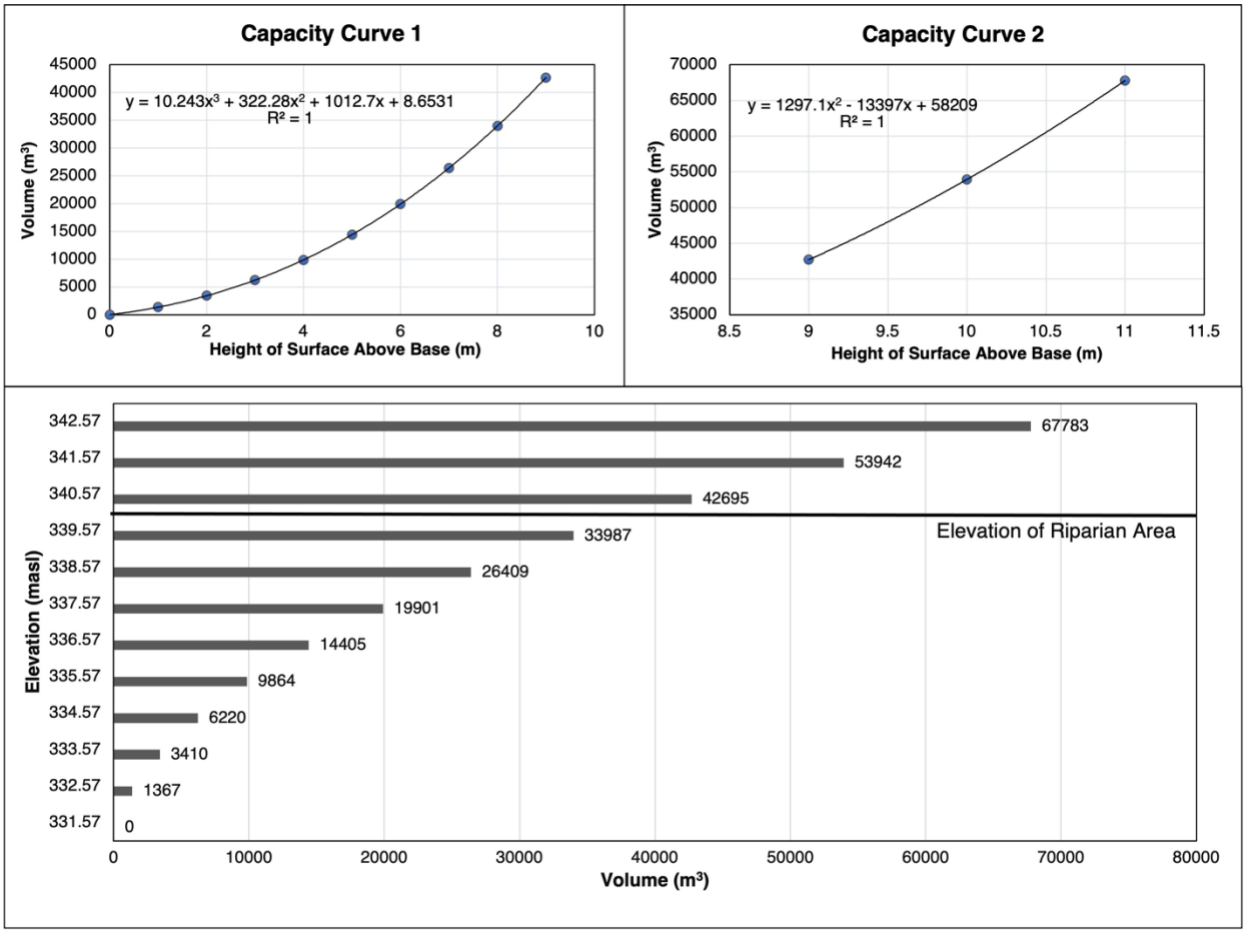


**Figure 2:** Volume calculations and capacity curves for Lake Miwasin, Fort McMurray, Alberta. Curve 1 represents the volume of the basin below the littoral zone. Curve 2 represents the volume of the basin above the littoral zone, which begins 9 m above the bottom of the basin at an elevation of 340.5 masl.

### *2.4.1 Water Balance*

Surface water inflow was intermittent throughout 2020 and 2021, driven by rainfall on the uplands (Figure 3). In 2020, there was a total of 500 mm of rain recorded between May 1 and October 13. The inflow during 2020 was characterized by periods of high discharge (0.8 L/s) separated by periods of low discharge (<0.8 L/s) (Figure 3). Periods of high discharge were

classified into nine events and details about the duration and associated volumes are displayed in Table 1. The total volume of surface water inflow for 2020, including both low and high discharge periods, was 12,918 $m^3$.

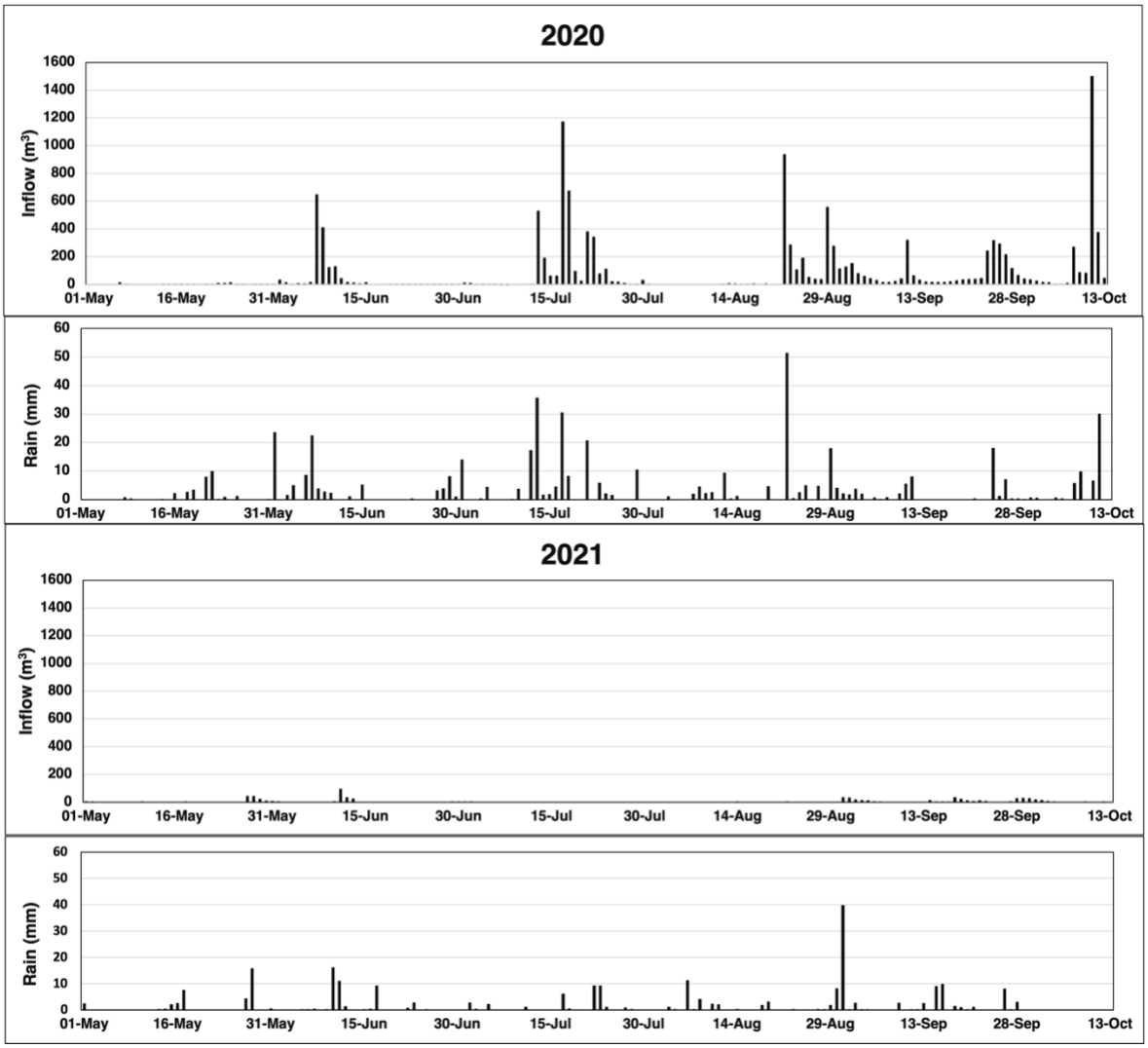


**Figure 3:** Rainfall and surface water inflow for Lake Miwasin, Fort McMurray, Alberta in 2020 and 2021.

In 2021, rainfall between May 1 and October 13 was only 227 mm, resulting in little surface inflow (Figure 3). No water was observed flowing through the inlet from June 14 to August 29, 2021, therefore any recorded inflow during this period has been assumed to be an error. Total surface

water inflow from May 1 to October 13, 2021, was only ~5% of surface water inflow observed during the same period in 2020 (627 $m^3$; Figure 4).

Evaporation was higher than precipitation for both years, with totals from May 1 – October 13 of 508 mm and 482 mm for 2020 and 2021, respectively. The total volume of water lost due to evaporation, along with that added from direct precipitation onto the lake, were calculated using the surface area corresponding with the average water level for each year (Figure 4). Average surface areas for 2020 and 2021 were 12,430 $m^2$ and 11,815 $m^2$, respectively. In 2020, surface water inflow and outflow were the largest components of the water budget, whereas in 2021, evaporation was the dominant flux term resulting in a decrease in the volume of the water cap over the study season, represented by the negative change in storage (Figure 4).

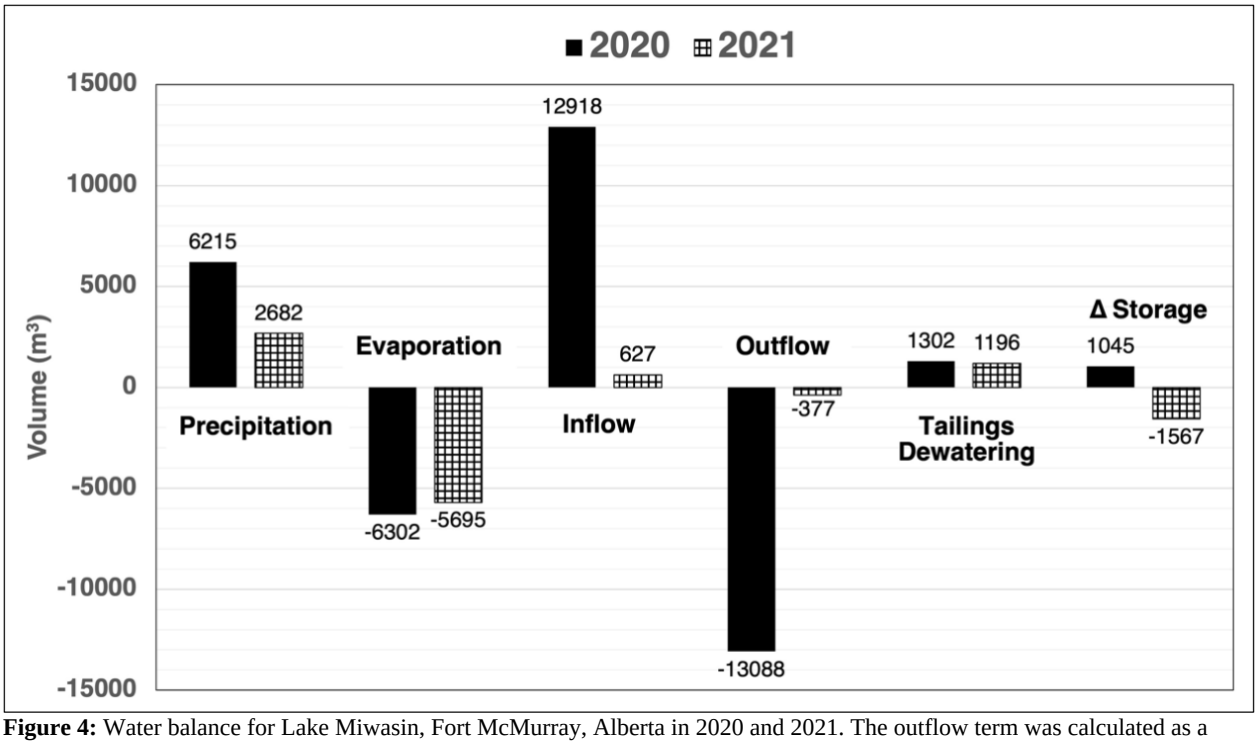


**Figure 4:** Water balance for Lake Miwasin, Fort McMurray, Alberta in 2020 and 2021. The outflow term was calculated as a residual.

The lake surface elevation had a recorded change of 2 cm between the start and end of the 2020 study season. Fluctuations throughout the summer months were observed as the water level

dropped by 8 cm to reach its lowest level on July 9 and rose by 16 cm to reach the maximum level on October 11. Daily averages of the mudline elevation for 2020 showed a decrease in 23 cm over the study season resulting in a volume of 1,302 $m^3$ being released to the water cap from tailings dewatering. The average lake surface and mudline elevation for the 2020 study season were 341.67 and 337.26 masl, respectively, yielding an average lake volume of 37,124 $m^3$.

During 2021, the lake stage continually decreased over the study season resulting in a 29 cm drop from May – October. The mudline elevation also decreased by 22 cm resulting in a volume of 1,196 $m^3$ released to the water cap from tailings dewatering. The average lake surface and mudline elevation for the 2021 study season were 341.39 and 337.08 masl, respectively, yielding an average lake volume of 34,646 $m^3$.

### *2.4.2 Residence Time with Tonolli's Model*

With the water level in 2021 being lower than the outlet culvert and the significant decrease in volume over the study season, the assumptions required to apply Tonolli's model were not met. Therefore, the following section offers a residence time estimate for the 2020 season only.

Surface inflow in 2020 was separated into nine different events where discharge was classified as high (> 0.8 L/s). Low discharge values (< 0.8 L/s) were neglected here to allow for more efficient categorization and delineation of events. This reduced the total volume of surface water inflow over the 2020 season from 12,918 $m^3$ to 11,535 $m^3$. The change in lake volume was also considered negligible over the study period, and the seasonal average volume of 37,124 $m^3$ was kept constant as is required for CSTR conditions (Levenspiel, 1998).

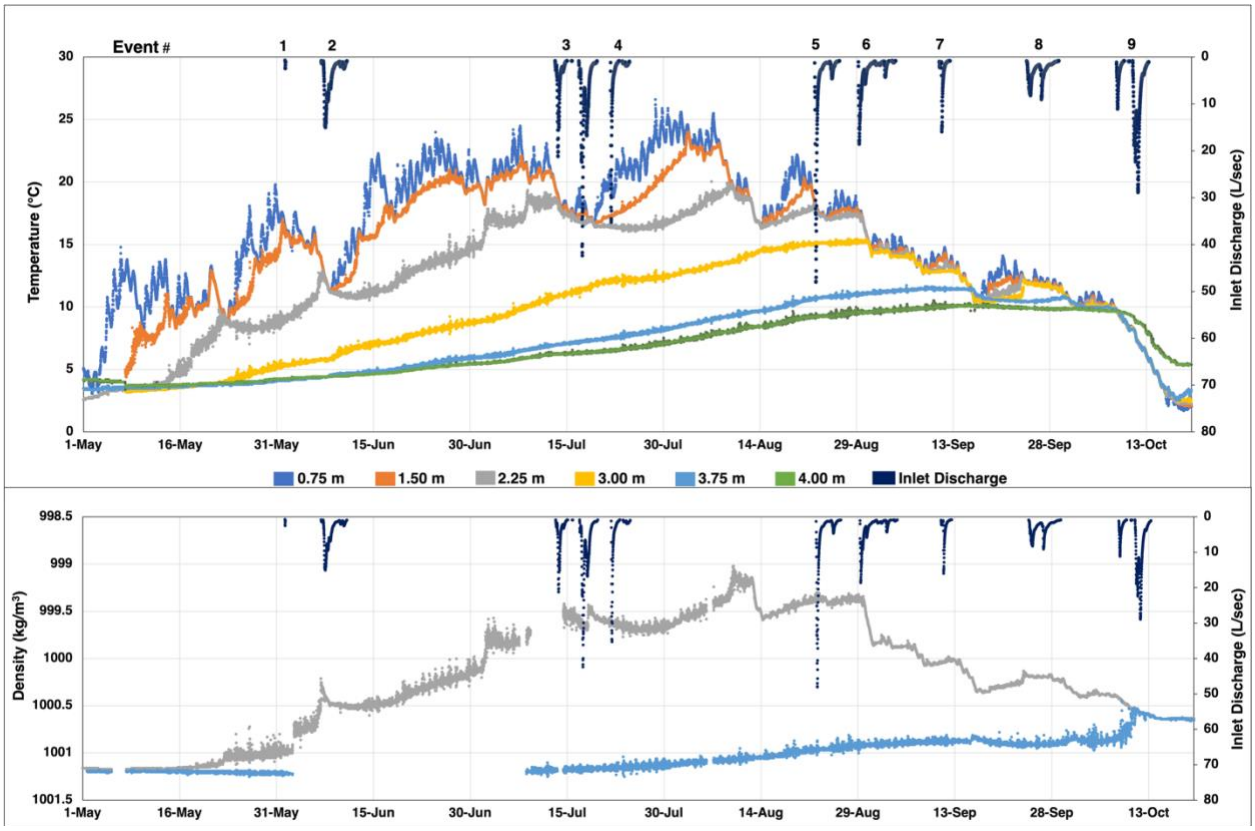


**Figure 5:** Lake Miwasin water cap (2020) temperature profile (top) and density (bottom). Surface inflow events from upland runoff are included in each plot on the secondary y-axis.

Temperatures below 3 m increased gradually and consistently from the middle of May until the end of August, while temperatures at 2.25 m and above were susceptible to periods of rapid fluctuation (Figure 5). During events 2, 3, 4 and 5, water temperature in layers 1, 2 and 3 became temporarily isothermal before warming and further separating. Approximately halfway through event 6, the water temperature in the surface layers dropped and layers 1-4 became isothermal and stayed such until the end of event 7. By October, the entire water column was nearly isothermal, except for slightly warmer temperatures in the deepest layer.

Water density was roughly the same at depths of 2.25 m and 3.75 m at the beginning of the study season but started to decrease at 2.25 m around the end of May. The density at 2.25 m continued to decrease until August 10$^{th}$ at which time a density difference of 2 kg/m$^3$ existed between the

water at depths of 2.25 m and 3.75 m. The density at 2.25 m then started to increase over the rest of August and September until equalizing with the 3.75 m depth around the 10th of October.

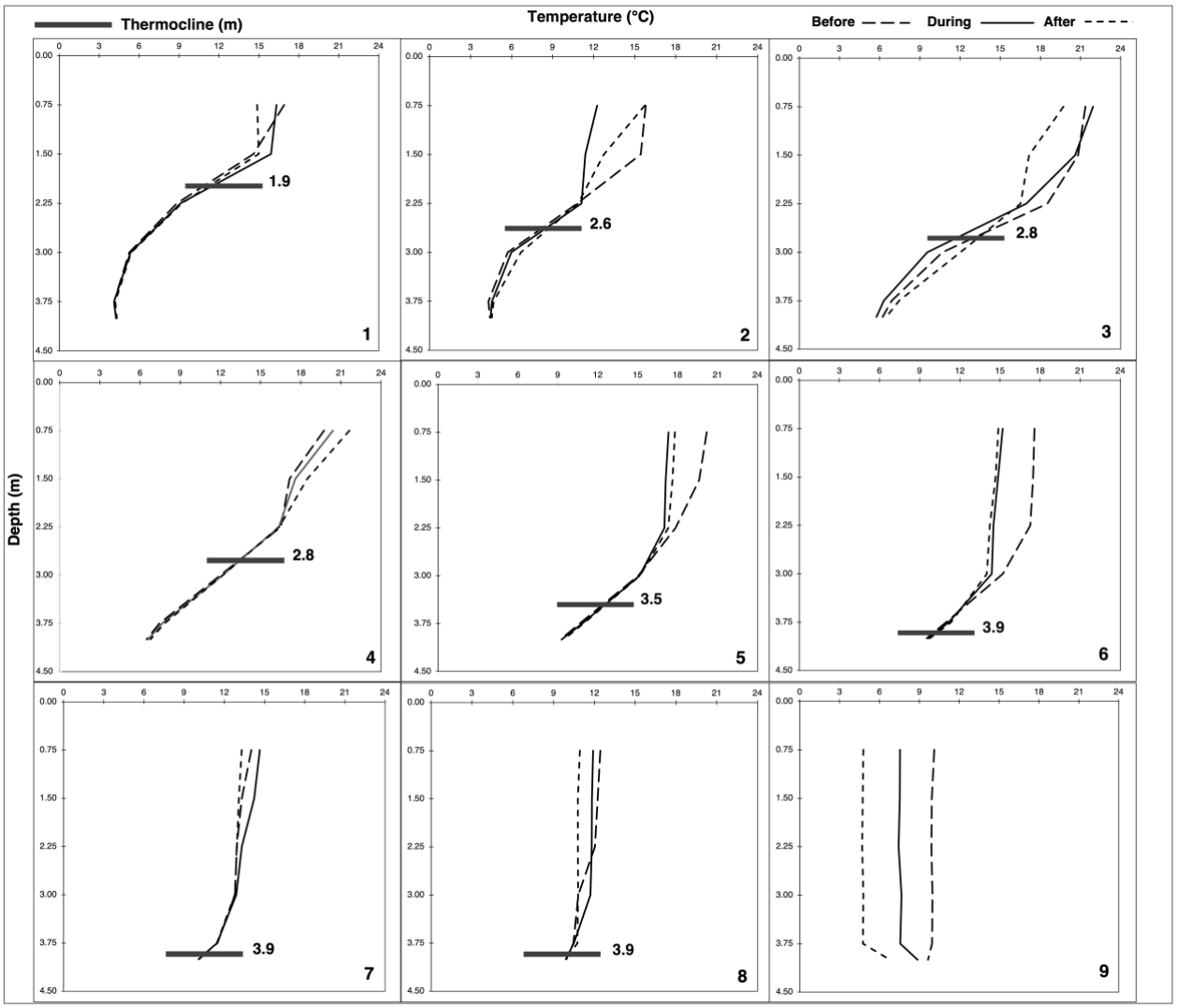


**Figure 6**: Thermal profiles of the 2020 Lake Miwasin water-cap. Events numbers are indicated in the bottom right corner of each plot and correspond to the dates and times displayed in Table 1. Each plot has three lines associated with the thermal profile at different stages surrounding the indicated event. 'Before' represents the temperature profile 24 hours before the inflow event began, 'During' is the profile in the middle of the event, and 'After' represents the thermal profile 24 hours after the end of the event. Each point represents the average of 10 sequential 15-minute measurements (i.e., 2.5 hr average).

A seasonal thermocline was present during events 1 - 8, and the depth of the thermocline can be seen to increase from May to September (Figure 6). Water temperatures below the thermocline stayed consistent during most of the events, with the exceptions of events 2 and 3 where the layers

beneath the thermocline became warmer after the event (Figure 6). The position of the thermocline also dropped during a couple of events; most notable was event 2 with a 60 cm drop, and event 6 with a 40 cm drop from the depth prior to the event. Thermocline depths displayed in Figure 6 are the deepest positions measured either before, during or after each event. Depths of the stated thermoclines were used to delineate the bottom of the mixed layer for each event (Table 1).

**Table 1:** 2020 Surface water inflow events. Events are numbered sequentially from the earliest date of occurrence, and a discharge value of 0.8 L/sec was used as a threshold to identify events. If discharge values dropped below 0.8 L/sec for longer than 48 hours, future inflow was determined to be a new event. The water temperature was averaged over the event period to determine the average temperature of inflow. The mixed layer volume was determined as the volume of the water cap above the thermocline depth associated with each event (Figure 5). $C_o$ is the fraction of old water in the mixed layer after the event has ended. $V_{OM}$ represents the volume of old water in the mixed layer after the event has ended.

| Event | Start Date | Duration (hr) | Volume of Inflow ($m^3$) | Inflow Temperature (°C) | Mixed Layer Volume ($m^3$) | $C_o$ ($m^3$) | $V_{OM}$ ($m^3$) |
|---|---|---|---|---|---|---|---|
| 1 | June 1 | 2 | 12 | 12 | 19,647 | 0.99 | 19,635 |
| 2 | June 6 | 95 | 1297 | 11 | 24,524 | 0.95 | 23,281 |
| 3 | July 13 | 156 | 2674 | 16 | 25,684 | 0.86 | 22,136 |
| 4 | July 21 | 70 | 849 | 19 | 25,684 | 0.83 | 21,428 |
| 5 | August 22 | 92 | 1542 | 16 | 28,927 | 0.81 | 23,422 |
| 6 | August 29 | 138 | 1275 | 12 | 30,209 | 0.78 | 23,704 |
| 7 | September 10 | 40 | 379 | 12 | 30,209 | 0.77 | 23,410 |
| 8 | September 24 | 119 | 1189 | 10 | 30,209 | 0.75 | 22,523 |
| 9 | October 8 | 119 | 2318 | 3 | 37,124 | 0.75 | 27,708 |

The volume of the mixed layer increased throughout the season, eventually encompassing the entire water cap at the beginning of October. $V_0$ within the lake decreased to 75% of the initial volume by the end of the season, resulting in a final volume of 27,708 $m^3$. Total volume of old water lost over the study period was 9,416 $m^3$. If the inflow and outflow dynamics were held constant to the measured values for the 2020 open water season, and only the hydrologic fluxes during the open water season are considered, the initial volume of Lake Miwasin would decrease by 63% after ~ 2.5 years. This is also equal to the residence time of a conservative substance using the above stepwise approach and assuming CSTR conditions within the mixed layer.

## 2.5 Discussion

### *2.5.1 Water Balance*

Precipitation and evaporation heavily influence the water balance of pit lakes, and a high degree of scrutiny should be applied when modeling the effects of a changing climate on the hydrology of these constructed systems (Grimaldi, 2009). Some modeling has been used to simulate scenarios of both water scarcity and water abundance for pit lake planning and design (Aquanty Inc., 2020). However, research on pit lake hydrology in the AOSR has been limited by a lack of study sites. Lake Miwasin presents an opportunity to observe how changes in precipitation impact the hydrology within a constructed lake and catchment complex, and the stark contrast in precipitation between 2020 and 2021 resulted in decreased surface inflow and a significant drop in lake surface stage. Average annual precipitation for the Boreal Plains is ~ 480 mm, 70% of which (i.e., ~336 mm) occurs as rainfall in the summer season (Devito et al., 2012), indicating that summer rainfall in 2020 was an above-average year with 500 mm, and 2021 below average with 227 mm. Surface water inflow at Lake Miwasin during the summer season is directly controlled by rainfall, with the low amount of rainfall received over the 2021 season resulting in an absence of surface water inflow into the lake. In addition to the low precipitation, the drop in the surface water level in 2021 also stems from the lack of groundwater interaction. Groundwater flow-through can help offset losses from evaporation during periods of low precipitation within the Boreal Plains as the sustainability of open water bodies in this region is often dependent on connectivity with large groundwater systems (Smerdon et al., 2005). Ongoing research is being completed on the hydrology of Lake Miwasin uplands; however, no groundwater interaction has been identified between the lake and the surrounding landscape thus far.

Evaporation is an important hydrologic process throughout the Boreal Plains, as open water bodies in this region tend to have high evaporation rates and function as evaporation windows on the landscape (Devito et al., 2012). Evaporation values for Lake Miwasin were slightly lower than those reported for BML between May 1 and October 31, which averaged 544 mm from 2013 to 2019 (Clark et al., 2021), likely due in part to their difference in size (BML is 780 ha, while Lake Miwasin is 1.2 ha). Evaporative losses from large lakes have been estimated to be higher than small lakes within the same geographic setting due to higher wind speeds caused by a longer fetch, and higher energy storage leading to lower Bowen ratios and postponed ice cover enabling evaporation to occur later in the year (Wang et al., 2019). Energy storage in lakes is correlated with depth (Gorham, 1964) and Lake Miwasin has a high depth to surface area ratio compared to natural boreal lakes. Out of 40 lakes surrounding Fort McMurray that have been monitored as part of a regional program, only five have a greater maximum depth than Lake Miwasin even though the lake with the smallest surface area is 3 times greater than that of Lake Miwasin (Bennett et al., 2008). Oil sands pit lakes may have other unique attributes that affect evaporation, such as the presence of a surface hydrocarbon sheen as observed at BML (Clark et al., 2021). Further research is needed to estimate how evaporation rates will vary between Lake Miwasin and the future commercial-scale UPL.

Studies of water balances and residence times are often completed over a hydrologic year (November 1 to October 31) to include shoulder season events such as snowmelt, an important hydrologic component in the Boreal Plains (Ketcheson and Price, 2016). Although the Boreal Plains are typically in a net annual water deficit, the accumulation of snow can lead to a water surplus at the end of the winter season (Devito et al., 2012), which is distributed throughout the landscape during the snowmelt. Surface inflows to Lake Miwasin have been observed in the field

during spring freshet, and previous research in the AOSR indicates a large portion of snowmelt water can travel as overland flow in reclaimed landscapes (Ketcheson and Price, 2016). Snowmelt is expected to introduce a significant amount of surface flow to Lake Miwasin during the spring season, thus affecting both water balance and residence time estimates. Although future research efforts should focus on this potentially important annual source of freshwater for pit lakes, it was beyond the scope of the current study.

Water balances are generally completed with a residual term to account for errors and un-measured fluxes. For example, over 2 consecutive years, Smerdon et al (2005) estimated residual terms of 8% and 7% of lake inputs in a Boreal lake in Alberta. Calculating the outflow as a residual term likely introduced errors in both the water balance and residence time estimate. For example, in 2021 the computed outflow/residual term is ~ 337 $m^3$ even though the water level in the lake was below the outlet culvert for the entire study season. As there was no surface outflow, the volume associated with the residual term was the product of errors in one or multiple of the other estimated water balance terms. During spring freshet, melt water from the parking lot north of the lake was observed entering the lake via the constructed boat launch, and this location may have resulted in un-measured additions to the lake during periods of heavy rainfall.

### *2.5.2 Residence Time with Tonolli's Model*

The Tonolli's model incorporates CSTR theory into residence time estimates for stratified lakes by only considering the volume of the mixed layer, delineated by the presence of a thermocline, as being diluted by surface water inflow during periods of stratification. As tailings deposits in pit lakes continue to settle and release process-affected water, increased concentrations of oxygen demanding substances, salinity, and dissolved organics may accumulate in the deeper layers of the water cap (Castendyk et al., 2012). This accumulation can contribute to meromictic

conditions (i.e., incomplete mixing), especially in lakes with winter ice cover and high meltwater inputs (Pieters and Lawrence, 2014). As hydrologic inputs to boreal lakes are small during the winter season, inflow events during the open water season will be an important source of fresh water. Applying a residence time model that considers both incomplete mixing of the water column and non-uniform dilution of the lake layers was thought to be a useful tool to understand how hydrology may be affecting outflowing water quality in a small system like Lake Miwasin, where short term event-based inflows and outflows were observed.

Future pit lakes in the AOSR are intended to be holomictic (i.e., periodic complete mixing) to minimize anoxic conditions and high salinity concentrations directly above the tailings-water interface (Castendyk et al., 2012) making them functionally similar to boreal lakes, which typically experience annual turnover (Gibson et al., 2002). The water column within Lake Miwasin was near isothermal at the beginning of May and in October but displayed a temperature gradient greater than 15 °C during June, July, and early August, indicating thermal stratification over the summer months (Figure 5). Rapid temperature fluctuations were observed above the seasonal thermocline indicating turbulent mixing, whereas the layers below the thermocline stayed thermally stratified. The slight increase in temperature in the layers below the thermocline during events 2 and 3 (Figure 6) may be an indication that the migration of warmer water across the thermocline had occurred. The average water temperature of inflow for event 1 was slightly lower than the thermocline, indicating the density of the inflowing water may have been greater than the water in the mixed layer. However, the inflow volume was small, and no temperature change was observed in the layers below the thermocline (Figure 6). If salinity concentrations in the inflowing surface waters are low and the average temperature is a fair representation of the density, flushing

of conservative species from the deepest lake layers directly above the mudline is likely limited during periods of thermal stratification.

Previous applications of Tonolli's model were completed on Lake Maggiore (surface area of 212 $km^2$, 372 m deep) and Lake Iseo (surface area of 60.9 $km^2$, 256 m deep) (Pilotti et al., 2014a), which are both substantially larger and deeper than Lake Miwasin. Research on thermoclines in small and shallow water bodies is limited; however, the formation of multiple thermoclines with varying degrees of strength has been documented in ponds (Touchart and Bartout, 2012) and shallow boreal lakes (Xenopoulos and Schindler, 2001). Thermoclines in shallow water bodies are generally less stable than thermoclines in deep lakes, with transient thermoclines often degraded during periods of mixing (Touchart and Bartout, 2012). The above analysis of the temperature profile surrounding each inflow event aided in the identification of the seasonal thermocline, meaning a thermal step that met the required density gradient and persisted during periods of mixing (Figure 6). As the maximum fetch at Lake Miwasin is short (~165 m) and the surface is sheltered by an encompassing berm (Figure 1), the extent of vertical mixing caused by wind is expected to be low compared with larger lakes (Petrone et al., 2007). Surface water inflow can also alter thermal stratification, especially when the volume of inflow is large compared to the volume of the lake (Wetzel, 2001). The effects of wind and surface water inflow on mixing at Lake Miwasin were not differentiated here, as temperature changes were assumed to track the extent of mixing caused by all drivers.

One limitation in the current study is that temperature was used as the sole driver of differences in water density and mixing. In hydrodynamic modeling, temperature, salinity, dissolved oxygen, and phytoplankton are all considered appropriate constituents for model calibration and using temperature alone can cause issues as it is non-conservative (Cole and Wells, 2003). Salinity

measurements were only collected at depths of 2.25 m and 3.75 m resulting in insufficient data to construct a full profile. Salinity can have a large effect on water density, and lakes that develop salinity gradients may resist complete mixing even if the entire lake becomes isothermal (Castendyk et al., 2012). Future studies on mixing in pit lakes could benefit from collecting multiple profiles of the above-mentioned hydrodynamic calibration constituents; however, cost and instrumentation availability are limiting factors. Although temperature does not solely explain water density and reflect hydrodynamic processes, changes in temperature are regularly used to identify large mixing patterns in lakes and were thus applied here to estimate mixing events within Lake Miwasin.

The application of Tonolli's model to Lake Miwasin and resulting residence time estimate were limited by the high number of assumptions required to apply CSTR conditions to a stochastic system. The initial applications of the model were completed for oligomictic lakes where complete mixing throughout the entire water column was not occurring on a regular basis. As the temperature profile at Lake Miwasin is indicative of dimictic conditions, complete mixing of the water column is likely to occur during the spring and fall seasons, resulting in regular dilution of conservative species from the deeper layers of the lake.

## 2.6 Conclusion

Successful incorporation of pit lakes as permanent reclamation features in the AOSR requires they be self-sustaining with minimal future management. Lake Miwasin offers the first opportunity to study the hydrology of a pit lake in the AOSR within a constructed catchment where the volume of the water cap is not actively managed. During the open water seasons of 2020 and 2021, the surface water inflow to Lake Miwasin was controlled by precipitation falling on the adjacent

uplands. High levels of precipitation during 2020 caused flow-through conditions where large volumes of freshwater were supplied to the lake resulting in the lake being diluted by ~ 25 %. Conversely, low levels of summertime precipitation in 2021 resulted in minimal freshwater additions to the lake and functional terminal flow conditions with evaporation as the only hydrologic output. As the success of oil sands pit lakes relies on the establishment of hydrologic connectivity with the surrounding landscape, the sustainability of these constructed systems will be heavily influenced by future climatic conditions.

# Chapter 3 – The Energy Balance

## 3.1 Introduction

Over 50 years of surface mining in the Athabasca Oil Sands Region (AOSR) of Alberta, Canada has generated large mined-out voids in the landscape, referred to as pits, and a by-product waste called tailings (Alberta Energy Regulator, 2020). Pit lakes are a widely applied reclamation technology employed to both reclaim mine pits and sequester tailings (Golder Associates, 2017) and have been studied in the AOSR for over 40 years (COSIA, 2021). Currently, only two oil sands pit lakes exist in the AOSR: Base Mine Lake (BML), which is a full-scale (780 ha) pit lake located within Syncrude Energy's Mildred Lake Mine lease; and Lake Miwasin, a pilot scale (1.2 ha) pit lake located within Suncor Energy Inc's Base Mine lease. Although proposed oil sands pit lakes will vary in physical characteristics, composition of freshwater, and accommodation of fluid tailings (FT), all oil sands pit lakes are intended to contribute to restoring the landscape to a locally representative Boreal ecosystem (COSIA, 2021).

Lakes are important landscape features in Boreal regions as they interact energetically with the surrounding environment serving as both heat sinks and sources (Oswald and Rouse, 2004). Most of the energy exchange of a lake occurs at the water surface (Imboden and Wuest, 1995), with the primary source of heat being solar radiation (Wetzel, 2001). The amount of heat a lake can absorb and store is a function of the morphometric characteristics such as surface area, depth, volume, and basin shape (Gorham, 1964). Once within a lake, energy plays an integral role in regulating the biological, physical, and chemical processes (Gianniou and Antonopoulos, 2007). Lakes lose energy at the surface both as sensible heat and through the latent heat required to drive evaporation (Imboden and Wuest, 1995). In northern regions, heat stored in lakes over the summer is generally

released back to the atmosphere in the fall, providing a source of convective energy during the onset of the winter season (Rouse et al., 2005).

One method used to relate energy storage within a lake to the rates of exchange with the surrounding environment is the energy balance (Sturrock et al., 1992; Winter et al., 2003). Initial applications of the energy balance came from the limnology field and were primarily focused on thermal energy stored within the water body (Forel, 1880; Wetzel, 2001; Touchart, 2016). The method later became important in hydrometeorological applications and was regarded as a reliable means of estimating lake evaporation (Sturrock et al., 1992; Rosenberry et al., 1993; Winter et al., 2003; Gianniou and Antonopoulos, 2007). The energy balance has provided insight for effective water resource management as long-term applications can highlight how lakes respond energetically to varying climatic conditions (Lenters et al., 2005; Elsawwaf and Willems, 2012). The method has also been applied to assess differences in thermal and hydrologic characteristics between small and large lakes located within the same geographic region (Rouse et al., 2005; Wang et al., 2019).

Previous studies on oil sands pit lakes in the AOSR have applied the energy balance to understand lake thermal dynamics and water fluxes (Chang, 2020; Clark et al., 2021). For example, Chang (2020) determined that the thermal regime of BML is representative of natural northern lakes, as stratification during the summer months was observed. High energy storage in the spring also preceded high energy release and evaporation in the fall (Chang, 2020; Clark et al., 2021). Several unique qualities were noted at BML as the presence of a hydrocarbon surface sheen potentially impacted evaporation rates (Chang, 2020; Clark et al., 2021), and deposited oil sands tailings exhibit different thermal properties than natural lake sediments (Dompierre and Barbour, 2017). Despite these unique inherent qualities, BML is expected to interact energetically with the

surrounding ecosystem in proportional ways to natural medium to large sized northern lakes (Clark et al., 2021).

This paper applied the energy balance method to Lake Miwasin, the smaller, pilot-scale oil sands pit lake. The objective was to measure the magnitude of energy fluxes and relate these fluxes to the change of energy stored in the Lake Miwasin water column to identify how the physical characteristics of Lake Miwasin impact the energetics of the system. The study was completed during the open water season (May – October) for two consecutive years with varying climatic conditions. This research aims to advance the knowledge previously developed on oil sands pit lakes by providing energetics data on a pilot-scale oil sands pit lake constructed in the AOSR.

## 3.2 Materials and Methods

### *3.2.1 Site Description*

Lake Miwasin is a pilot-scale oil sand pit lake constructed near Suncor Energy Inc's Millennium Mine as a scaled-down version of the planned Upper Pit Lake (UPL), located in the current Dedicated Disposal Area 3 (BGC, 2018a). In 2017, roughly 40 000 $m^3$ of treated tailings were deposited into the 12 m deep pit, with the base sitting 10 m above the Wood Creek Sand Channel aquifer (BGC, 2018b). By May 2020, the tailings had settled to a height of ~5.5 m above the bottom of the basin and a 4.5 m thick water cap with a maximum fetch of 165 m and a surface area of ~12 000 $m^2$ developed on top of the tailings. Surface water inflow is directed to the lake through a single channelized inlet connecting the lake to a constructed upland to the east. The uplands are ~ 9 ha, comprising three hummocks and four swales with developing vegetation. The west side of the lake sits ~20 m from a forested edge with an average tree height of 8.5 m. A littoral zone was constructed along the east side of the lake with an area of ~2600 $m^2$ and a 4% slope. The lake inlet

is situated within the littoral zone and is built up ~1 m above the water level. Surface water from the uplands flows through a v-notch weir plate and down a section of cobblestone into the lake. The lake outlet is a steel corrugated pipe penetrating through the pit wall near the lake's northwest corner and sits ~10.5 m above the pit base. The top of the pit walls are built up ~0.5 m from the surrounding ground level creating a berm on the north, west, and south sides preventing overland run-off into the lake. The top 5.5 m of the pit walls are also lined with a 60 cm thick compacted clay layer, which is expected to minimize exchange between the Lake Miwasin water cap and the surrounding groundwater system (BGC, 2018b).


**Figure 7:** Field photos from four locations on the perimeter of Lake Miwasin providing a view of: 1. The lake looking south from the northern shore; 2. The riparian area on the lake's eastern shore from the north. 3. The eddy covariance equipment extended above the water surface to the west from the dock on the eastern shore; 4. The western shore situated ~ 20 m from a forested edge.

### *3.2.2 Instrumentation and Data Collection*

#### *3.2.2.1 Lake and Climate Data*

Temperature thermistors were installed on five Instrument Poles (IP 1-5) at depths of 0.75, 1.50, 2.25, 3.00, 3.75, and 4.00 m. Temperature measurements were recorded every 15 minutes and averaged horizontally across available sensors to provide a temperature reading for the water cap at each associated depth. The temperature of the tailings was measured using a VWP2100 Vibrating Wire Piezometer (RST Instruments, Maple Ridge, British Columbia, Canada) located on IP 3 approximately 1 m below the tailings/water interface (mudline). Air temperature (Ta) and relative humidity (rH) were measured with a digital CS215 sensor (Campbell Scientific, Logan, Utah, USA). The Vapor pressure deficit (VPD) was calculated by using Ta to calculate the Saturated Vapor Pressure (SVP),

$$SVP = 610.78e^{\frac{Ta}{(Ta+237.3)17.2694}} \quad (4)$$

where *e* is Euler's number (2.71828). VPD was then calculated using rH with,

$$\text{VPD} = \frac{SVP}{1000}\left(1 - \frac{rH}{100}\right) \quad (5)$$

Net radiation was measured using a NR-LITE2 net radiometer (Kipp and Zonen, Delft, Netherllands) installed on a dock approximately 1 m above the water surface. Wind speed and direction were measured by an IRGASON Eddy Covariance station (Campbell Scientific, Logan, Utah, USA).

#### *3.2.2.2 Eddy Covariance System*

Turbulent fluxes were measured with an IRGASON (Campbell Scientific, Logan, Utah, USA) eddy covariance system. The IRGASON was stationed on a dock beside the inlet with the sensors extended over the lake surface at a height of approximately 1 m. Raw fluxes were sampled at a frequency of 20 Hz, and averaged over a half-hour, with the half-hour averages

saved on a CR1000x datalogger (Campbell Scientific, Logan, Utah, USA). All fluxes were corrected for density, sensor separation, time lag and coordinate rotation (double coordinate rotation was used) following common Fluxnet protocols (Webb et al., 1980; Kaimal and Finnigan, 1994; Foken and Leclerc, 2004; Aubinet et al., 2012). The resulting half-hour fluxes were then processed in a custom R-Software script, which filtered each half-hour to ensure that it had at least 80% of the high-frequency records and that there was no potential for dew formation on the IRGA lenses by either precipitation or by comparing the dew point temperature to Ta. Additional filtering removed values that were greater than ±3 standard deviations of a moving average, which consisted of 10 half-hour neighboring values; further filtering was completed to check for physically improbable values. The Kljun et al. (2015) footprint analysis was used to constrain the measured fluxes to be within 80% of the desired site boundaries, using their FFP R-functions. Thereafter, fluxes with a corresponding friction velocity ($u^*$) < 0.10 m $s^{-1}$ were removed from the dataset. The filtered energy fluxes were gap-filled using the MDS method outlined in Reichstein et al. (2005), where global radiation (Rg), VPD, and Ta were used as the gap-filling conditions.

## 3.3 Theory and Calculations

### *3.3.1 Heat Content*

The heat content of a lake is defined as the amount of energy in calories that would be released if the lake cooled from the current temperature to 0 °C (Wetzel, 2001). The heat content of Lake Miwasin was calculated by dividing the water cap into 6 horizontal layers, each containing a temperature thermistor at the approximate center. The volume of each layer was calculated using

the capacity curves displayed in Zabel et al. (2023). The heat content of each layer was calculated by the following formula (Wetzel, 2001),

$$H = M\ T_W\ s \tag{6}$$

where H is the heat content in thermochemical calories (cal), M is the mass of the water (g), $T_W$ is the water temperature (°C), and s is the specific heat capacity of pure water (1ca/g°C). The heat content of each layer was then summed to get the total heat content for the entire lake, which was then divided by the average surface area ($cm^2$) for each season ($1.243 \times 10^8$ for 2020; $1.1815 \times 10^8$ for 2021) to provide a value related to the lake surface area ($cal/cm^2$).

### *3.3.2 Energy Budget*

The energy budget was calculated using,

$$\Delta Q_s = Q_n - Q_e - Q_h + Q_A - Q_g \tag{7}$$

where $\Delta Q_s$ is the change in energy stored within the water body, $Q_n$ is net radiation, $Q_e$ is the latent heat flux, $Q_h$ is the sensible heat flux, $Q_A$ is the net energy advected into the water body, and $Q_g$ is the heat flux between the water body and the lake sediments (all expressed in $W\ m^{-2}$). Net advected energy is generally small enough to be considered negligible (Gianniou and Antonopoulos, 2007) and was left out of the completed energy budget. Since all the surface fluxes, sediment flux, and the energy stored within the water column were measured directly at Lake Miwasin, an open energy budget was completed with the residual term functioning as a measure of error.

### *3.3.3 Latent and Sensible Heat Fluxes*

Both the latent and sensible heat fluxes from the Lake Miwasin surface were measured using the IRGASON eddy covariance system. Eddy Covariance is widely used method of measuring surface energy fluxes from small lakes and waterbodies (Nordbo et al., 2011; Burba, 2013; Zhao et al., 2019) and operates by the basic Eddy Flux formula,

$$F = \overline{\rho_a}\,\overline{w's'} \tag{8}$$

where the flux ($F$) is equal to the average air density ($\rho_a$) (kg/m$^3$) multiplied by the average covariance between the instantaneous deviations in vertical wind speed ($w'$) and the dry mole fraction of the gas of interest ($s'$) (Burba, 2013). The dry mole fraction is the ratio of moles of the gas of interest to moles of the dry air (Burba, 2013). $Q_e$ was calculated using,

$$Q_e = L\,\rho_a\,\overline{q'w'} \tag{9}$$

where $L$ is the latent heat of vaporization for water (2.26x10$^6$ J/kg), and $q'$ is the dry mole fraction of water vapor (mmol/mol) (Nordbo et al., 2011). The sensible heat flux was calculated using,

$$Q_h = \rho_a\,c_{\rho a}\,\overline{Tv'w'} \tag{10}$$

where $c_{\rho a}$ is the specific heat of air at constant pressure (1004 J/kg/K), and $Tv$ is the virtual temperature (K) (Nordbo et al., 2011). Virtual temperature is the temperature where the density of a dry air parcel is equal to the density of the same parcel when moist (Betts and Bartlo, 1991).

### *3.3.4 Tailings Heat Flux*

The heat flux between lake sediments and the bottom layer of the water column can be calculated by using the following one-dimensional heat conduction equation (Brown, 1969; Fang and Stefan, 1996),

$$Q_g = -\lambda\left(\frac{\Delta T_s}{\Delta_z}\right)ws \tag{11}$$

where $\lambda$ is the thermal conductivity (W/m/K) of the sediment and $\left(\frac{\Delta T_s}{\Delta_z}\right)ws$ is the temperature gradient at the sediment-water interface. For the current study, $\left(\frac{\Delta T_s}{\Delta_z}\right)ws$ was calculated using the lowest temperature thermistor in the water column (4.00 m depth) and the shallowest temperature sensor within the tailings (approximately 1 m below the tailing-water interface). As FT produced from the oil sands are predominantly composed of process-affected water, residual bitumen, and

suspended mineral solids (Gosselin et al., 2010), $\lambda$ will be calculated using the following formula applied for BML from Dompierre and Barbour (2017),

$$\lambda = \lambda_s^{(fs)} \lambda_w^{(fw)} \lambda_b^{(fb)} \quad (12)$$

where $\lambda_s$ is the thermal conductivity of the solid particles (W/m/K), $\lambda_w$ is the thermal conductivity of the pore water (W/m/K), and $\lambda_b$ is the thermal conductivity of the bitumen (W/m/K). The thermal conductivity of each component is raised to the power of the volume fraction of that phase in the tailings, where *fs i*s the volume fraction of solids ($m^3/m^3$), *fw* is the volumetric water content ($m^3/m^3$), and *fb* is the volumetric fraction of bitumen ($m^3/m^3$). Values for $\lambda_s$, $\lambda_w$, and $\lambda_b$ are adopted from laboratory analysis completed on samples collected from BML (Dompierre and Barbour, 2017). The volumetric fraction of each phase was determined from samples collected from Lake Miwasin at a depth of 0.95 m below the tailings-water interface.

## 3.4 Results

### *3.4.1 Climatic Variation Over the Study Period*

Notable variations in temperature, precipitation, and relative humidity occurred between the 2020 and 2021 summer seasons (Table 2). 2020 was an exceptionally wet year with 501 mm of precipitation received during the study period; over double the amount received in 2021 (227 mm) and substantially higher than the 30-year normal (300 mm) for the Fort McMurray region. This caused higher monthly averages of relative humidity and lower monthly averages of vapor pressure deficit in 2020, especially in the months of June and July. The 2021 study period was comparatively hot and dry with temperature maximums reaching 39.7 °C in June and 37.3 °C in July. Monthly averaged temperatures in 2021 exceeded the 30-year averages for all months except May (Table 1), and monthly averages of $Q_n$ were also notably higher in May and June of 2021

with values of 119 W/m$^2$ and 114 W/m$^2$, respectively, compared to 109 W/m$^2$ and 106 W/m$^2$ for 2020.

**Table 2:** Monthly averages of temperature and relative humidity, along with total precipitation at Lake Miwasin during the study periods are compared to the 30-year climate normal (30 yr N) for the Fort McMurray region. The 30-year climate normal data was retrieved from Environment and Climate Change Canada (Government of Canada, 2023).

| | Average Temperature (°C) | | | Precipitation (mm) | | | Relative Humidity (%) | | |
|---|---|---|---|---|---|---|---|---|---|
| | 2020 | 2021 | 30 yr N | 2020 | 2021 | 30 yr N | 2020 | 2021 | 30 yr N |
| May | 10 | 10 | 10 | 29 | 35 | 34 | 46 | 40 | 40 |
| June | 15 | 18 | 15 | 92 | 42 | 73 | 54 | 43 | 46 |
| July | 18 | 19 | 17 | 161 | 33 | 81 | 58 | 47 | 51 |
| August | 17 | 16 | 15 | 115 | 76 | 57 | 59 | 52 | 51 |
| September | 10 | 12 | 10 | 51 | 41 | 39 | 61 | 60 | 52 |
| October | 7 | 6 | 2 | 53 | 0 | 16 | 66 | 48 | 58 |

### *3.4.2 Energy Storage*

The Lake Miwasin water cap became thermally stratified during both 2020 and 2021 (Figure 8), however, 2020 had a greater and more prolonged degree of stratification than 2021. In 2020, the top 3 layers of the water cap (0 – 2.25 m) warmed quickly during the early spring and continued to warm until early August, with the highest water temperature of 26 °C recorded on July 28. This date also represented the highest degree of stratification, as a 20 °C difference existed between the shallowest and deepest layers. Temperatures in the top 3 layers then began to cool in the middle of August until the entire water cap varied by less than 5 °C by the middle of September. Deeper layers of the water column (3 – 4 m) warmed gradually from the start of May until the middle of September, with the deepest layer reaching a maximum of 10 °C.

In 2021, warming of the entire water cap occurred early in the season with temperatures in the deepest layer rising above 10 °C by the end of May. Substantial stratification was present from the end of May until the beginning of August, and the highest degree of stratification was represented by a 15 °C difference between the shallowest and deepest layers on July 2$^{nd}$. This was also the date of the highest temperature measured during the 2021 season at 28 °C. The deepest layer continued to warm until the middle of August when temperatures reached 18 °C. From the middle of August

until the end of the 2021 study season, the temperature throughout the entire water cap varied by less than 5 °C.

The heat content reflects the temperature profiles for both years (Figure 8). During 2020, the maximum heat content occurred on August 6th and was 5785 cal/cm$^2$. During 2021, the maximum heat content was higher (6572 cal/cm$^2$) and occurred earlier (July 2nd).

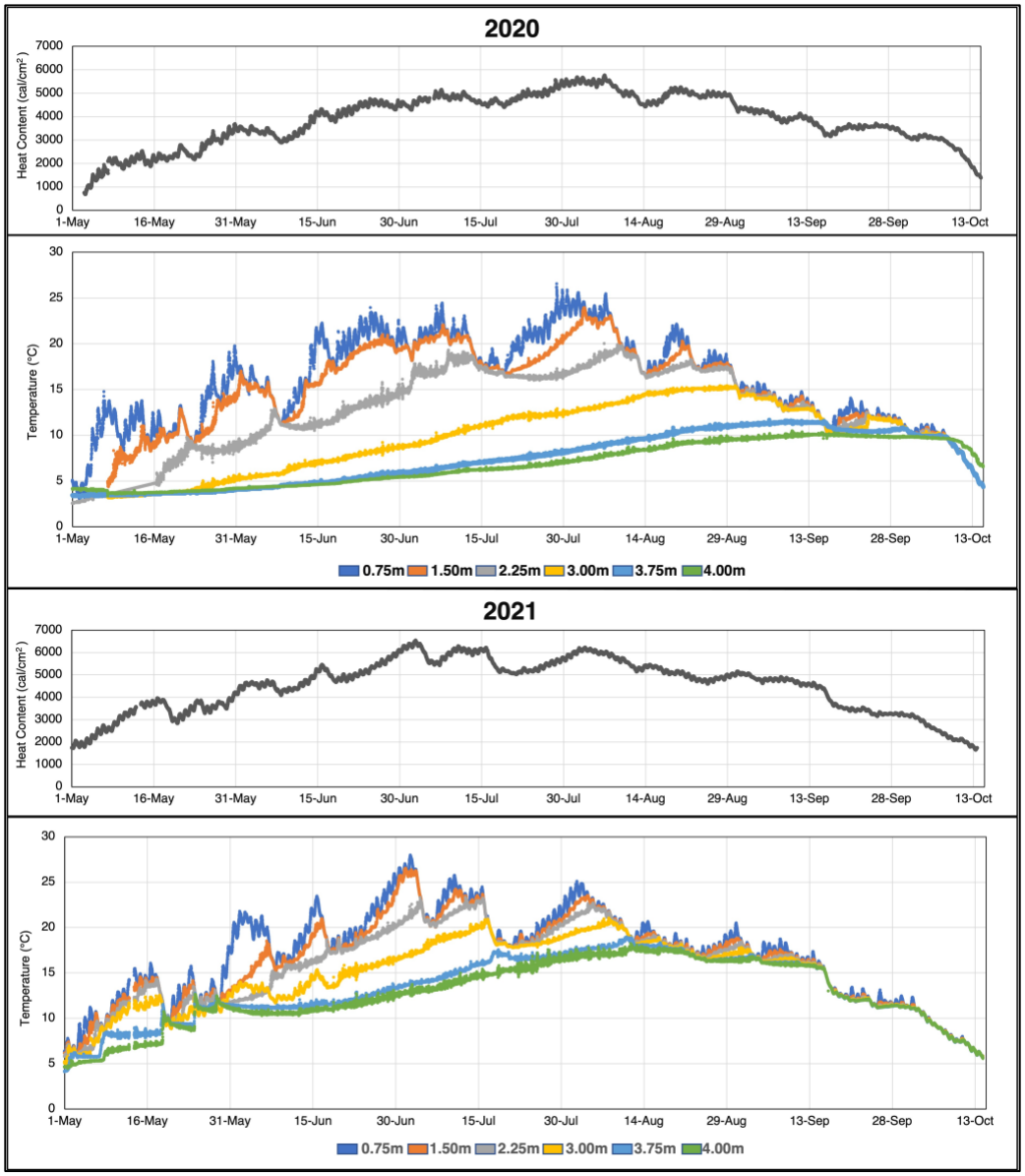


**Figure 8:** Temperature profiles and heat content of Lake Miwasin during the 2020 and 2021 study periods.

Rapid temperature fluctuations within the Lake Miwasin water cap were observed over both the 2020 and 2021 study seasons. Diurnal patterns in temperature were apparent, with these sinusoidal patterns most pronounced in the shallow layers decreasing in amplitude with depth. Along with the diurnal variations, there are also periods in both years when the temperature of the top several layers decreased substantially over the period of a few days. Examples are when the temperature at the 0.75 m depth dropped by ~ 9 ℃ from August 6 – 14, 2020, and in 2021 when the temperature at the 0.75 m depth dropped by ~ 7 ℃ from July 3 – July 6 (Figure 8). These decreases were most drastic during periods when the extent of thermal stratification was the highest and appeared to be restricted when the temperature gradient throughout the water column decreased (Figure 8). These drops in temperature also resulted in notable decreases in energy stored within both the shallow layers and the entire water cap.

To investigate the driving forces behind these fluctuations over daily timescales, energy stored within the top layer of the water column was regressed against several climatic variables and surface water inflow (Figure 9). Both air temperature and surface water inflow had negligible correlations with the change in energy on the daily time scale ($R^2 < 0.1$). Wind speed demonstrated a small correlation with an $R^2$ value of 0.23, and net radiation showed a moderate correlation with an $R^2$ value of 0.34.

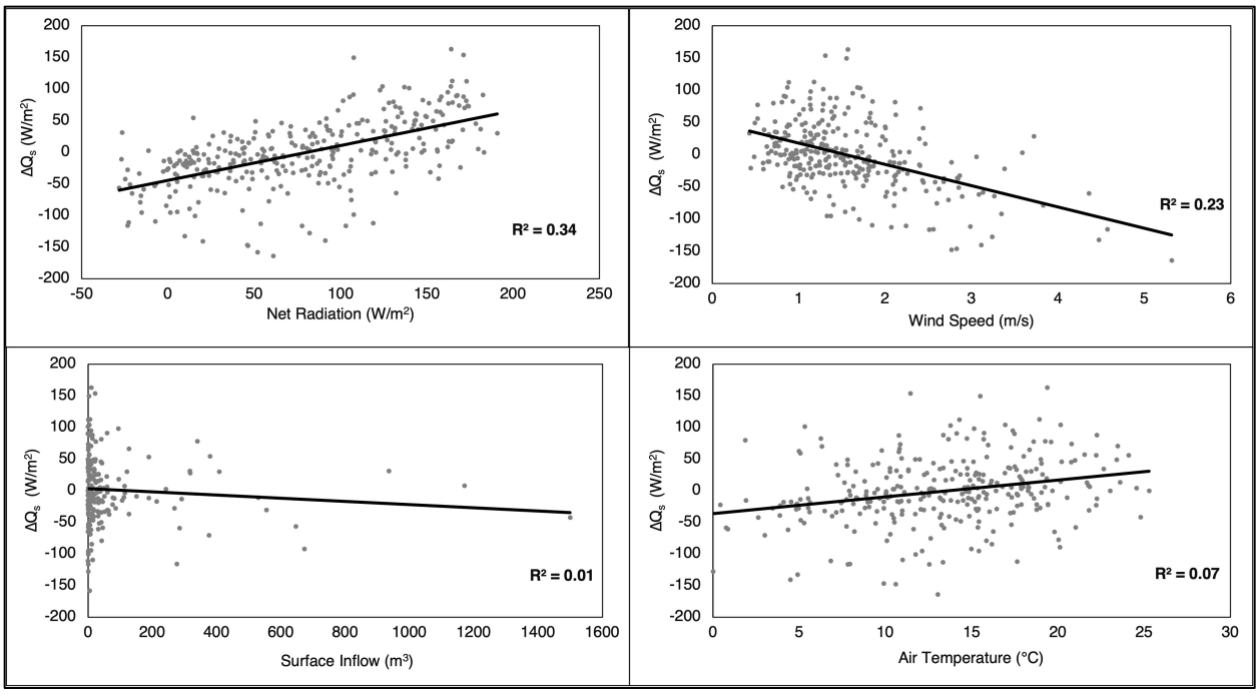


**Figure 9:** Changes in energy storage in the top layer of the water cap as a function of atmospheric conditions (net radiation, windspeed and air temperature) and surface water inflow. Each point represents a 24-hour average value.

### *3.4.3 Surface Energy Fluxes*

The latent heat flux varied on a diurnal basis with the highest values occurring in the late afternoon and the lowest values occurring during the night (Figure 10). Daily averages for both 2020 and 2021 ranged from 5 – 115 W $m^{-2}$ with the highest values occurring in June of each year. 2021 had higher values in general with monthly averages exceeding those of 2020 in all months except September. The sensible heat flux also varied diurnally, with the highest values observed during the late morning with low nighttime values often dropping into the negatives during the later summer months as the temperature gradient from the water column to the lower atmosphere reversed (Figure 10). Daily averages ranged between -20 and 50 W $m^{-2}$ for both years, although the values were generally higher in 2020 with monthly averages exceeding those in 2021 for every month except May.

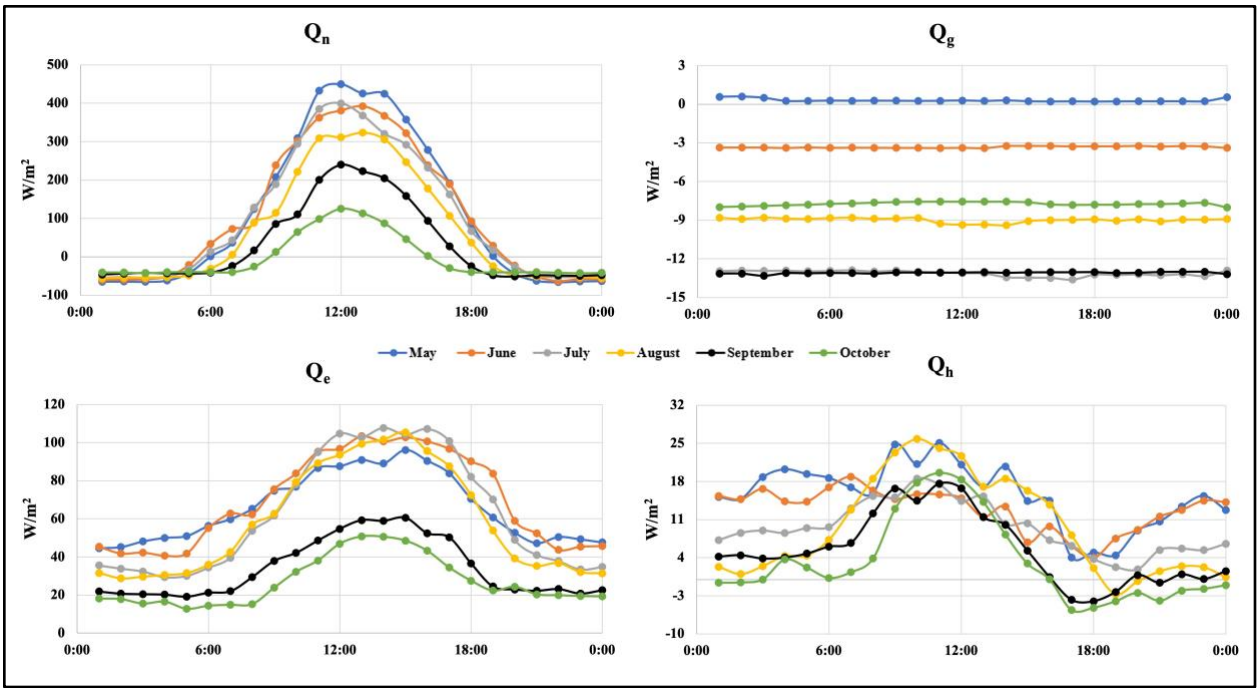


**Figure 10:** Surface and sediment energy flux components from both 2020 and 2021 averaged for time of day.

To assess the primary factors contributing to the latent heat flux at Lake Miwasin, values were compared with the vapor pressure (VPD), horizontal wind speed (U), and energy stored within the top layer of the water column ($H_{L1}$) on both half hour and daily timesteps (Figure 11). On both timescales, the $R^2$ values indicate either a negligible or low correlation for U and $H_{L1}$. For the VPD, the $R^2$ values indicate a moderate correlation on both the half hour and daily timescales.

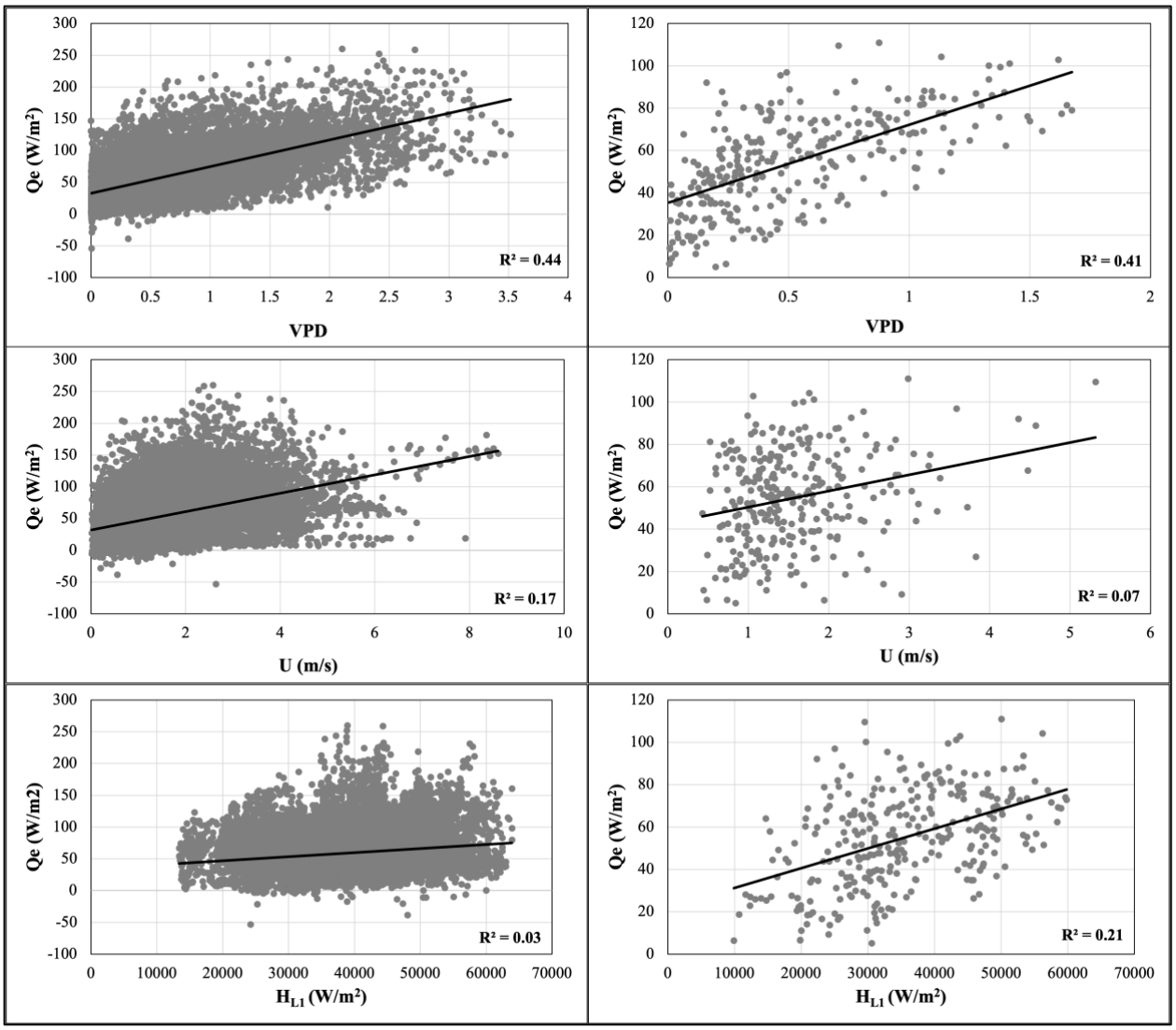


**Figure 11:** Latent heat flux plotted against the VPD, horizontal wind speed (U), and the energy stored within the top layer of the water column ($H_{L1}$) on both the half hour (left) and daily (right) timescales.

To assess the primary factors contributing to the sensible heat flux at Lake Miwasin, values were compared to the product of the temperature gradient between the water column and the lower atmosphere ($T_w - T_a$) and the horizontal wind speed (Figure 12). Only a small correlation was observed on the 30-minute timescale ($R^2 = 0.27$), with the correlation increasing to moderate for the daily timescale ($R^2 = 0.55$).

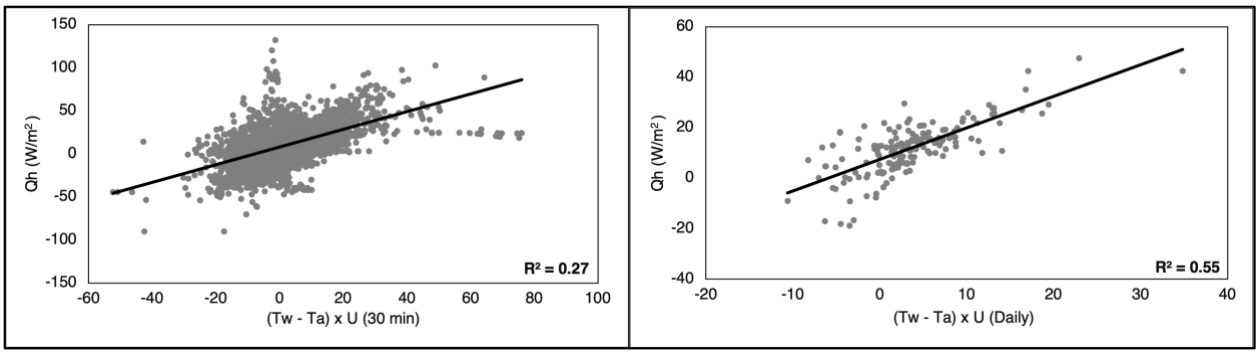


**Figure 12:** Sensible heat flux plotted against the temperature gradient between lake surface (Tw) and the air (Ta) multiplied by the horizontal wind speed (U) on both the half hour (left) and daily (right) timescales.

### *3.4.4 Tailings Heat Flux*

Values for the thermal conductivity (W/m/K) of $\lambda_s$ (3.10), $\lambda_w$ (0.57), and $\lambda_b$ (0.17) were adopted from Dompierre and Barbour (2017). Laboratory analysis of samples collected from the Lake Miwasin tailings deposit in August of 2020 determined *fs*, *fw*, and *fb* at a depth of 0.95 m were 0.65, 0.33, and 0.02, respectively. The thermal conductivity for the Lake Miwasin tailings was then calculated as 1.67 W/m/K using equation 12.

Low temperatures in the water column early in 2020 resulted in the tailings acting as a heat source (i.e., flux from the tailings to the water cap) until water temperatures rose and the gradient reversed in the middle of June (Figure 13). For the remainder of the 2020 study season, and the entire 2021 season, the temperature of the tailings was lower than the temperature at the base of the water column resulting in an energy flux to the tailings from the water column.

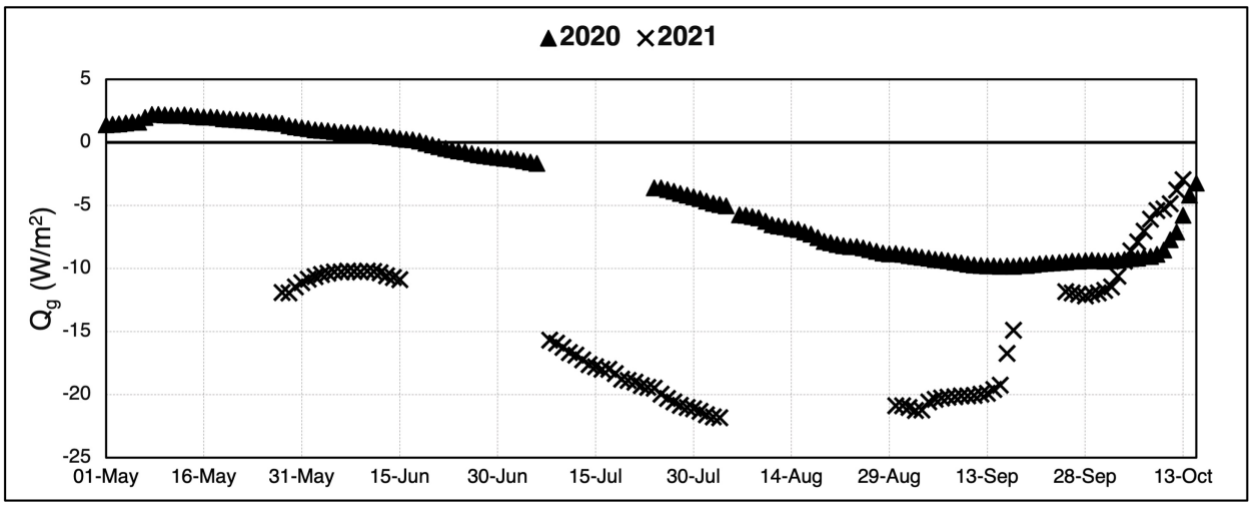


**Figure 13:** Daily average heat flux between the deposited tailings and the bottom layer of the water cap. Positive values represent heat migration from the tailings into the water cap and negative values represent heat migration from the water cap into the tailings deposit.

### *3.4.5 Energy Balance*

The energy balances for both the 2020 and 2021 study seasons are displayed in Figure 14. The values for $\Delta Q_s$ were graphed as reciprocals of the calculated values where months with negative values represent an average increase in energy stored within the water column and positive values represent an average decrease. For both 2020 and 2021, $\Delta Q_s$ shifted from a net increase to a net decrease in the same month as the maximum heat content occurred (August for 2020 and July for 2021). The residual values from the energy budget (Figure 14) are a consequence of calculating an open energy budget and were used as a measure of error for each month as positive values represent an excess of energy unaccounted for by the other terms and the negative values represent an over-allocation of energy by the other terms. For both 2020 and 2021, October had the highest residual value, followed by May with the second highest. These months also represented the greatest rates of change in energy storage within the lake, as October had the highest energy release rate from the lake to the atmosphere while May had the highest absorption rates by the lake from the atmosphere.

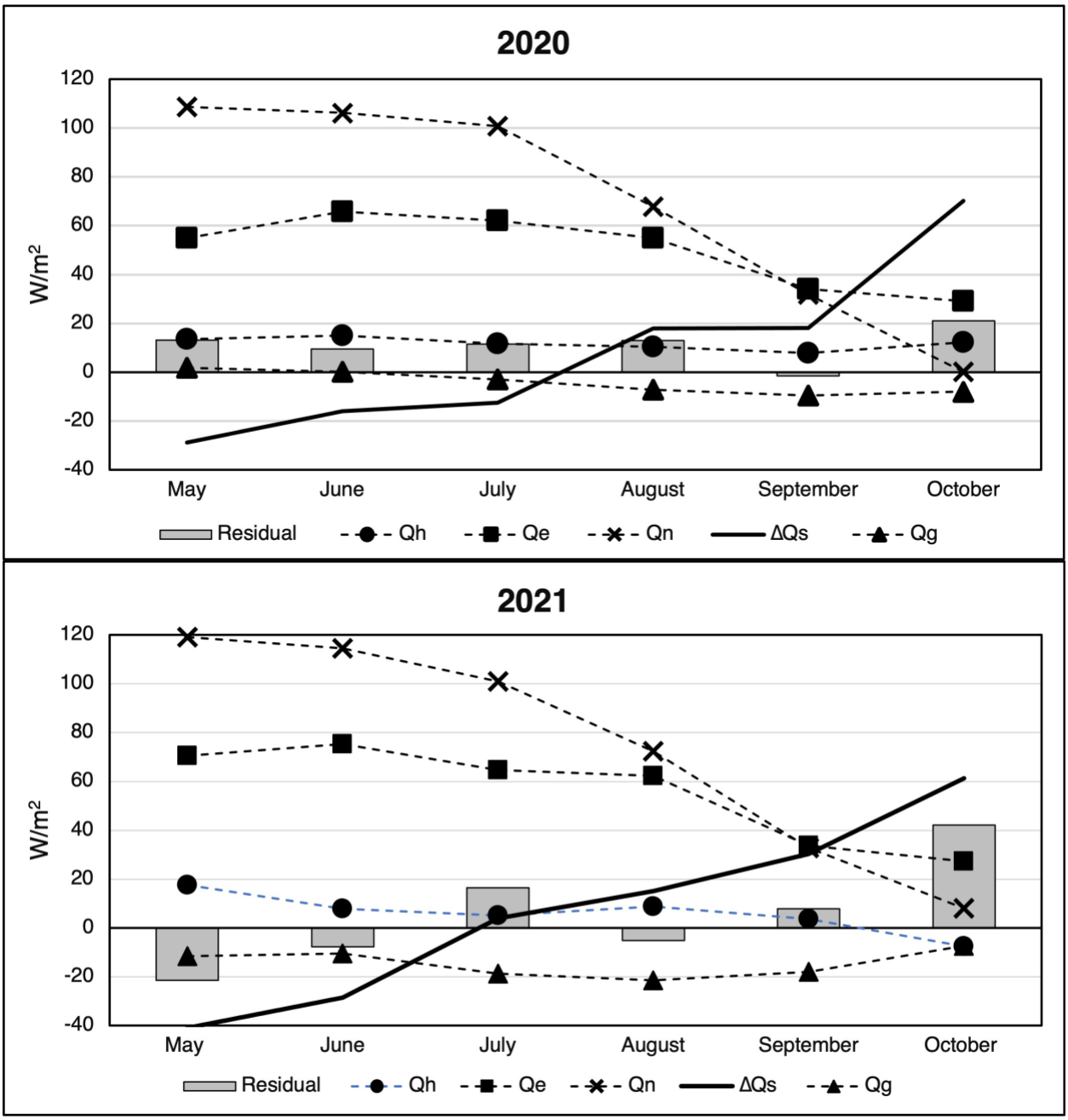


**Figure 14:** Monthly average values of the energy balance components. The values for $\Delta Q_s$ are graphed as reciprocals of the calculated values with positive values in the graph representing a decrease of energy within the water column.

The total energy balance terms for both study seasons are displayed in Figure 15. Net radiation was higher in 2021 contributing to warmer water temperatures in the deepest layer of the water cap resulting in a larger energy flux into the deposited tailings compared to 2020. Although high net radiation in the early months of 2021 led to the highest recorded water temperatures, the

early onset of the maximum heat content resulted in a longer period of energy loss and a lower change in net energy storage over the season compared to 2020. The Bowen ration was also higher in 2020 as there was a larger overall sensible heat flux and lower latent heat flux compared to 2021.

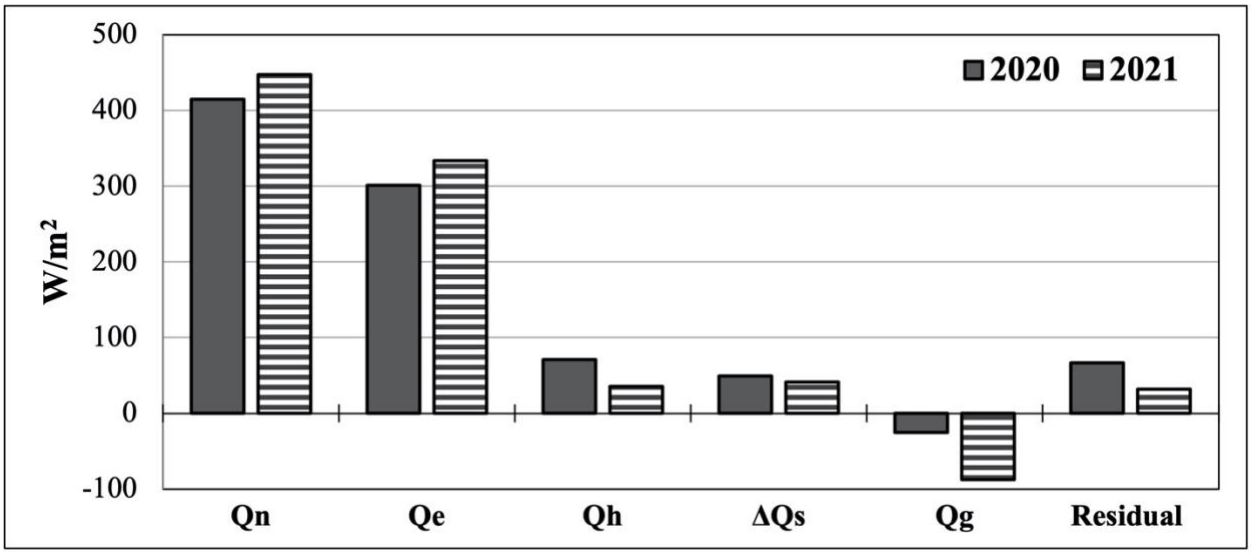


**Figure 15:** Annual energy balance terms for 2020 and 2021. Values represent the sum of monthly averages for each study season.

### *3.4.6 Wind Effects*

Wind speed and direction measurements collected approximately 1 m above the lake surface are compared with measurements collected on top of the east hummock in the constructed uplands in Figure 16. At the lake surface, the dominant wind directions are south and north, while winds from the west and east directions are the least common. On top of the hummock, the dominant wind directions are east and west while the least common directions are southwest and northeast. Wind speed is also slightly higher on top of the hummock compared to the lake surface, however wind speeds rarely exceeded 6 m/s at either location. Data included in Figure 16 is from the 2020 study season only as no data from the upland's location was available from 2021.

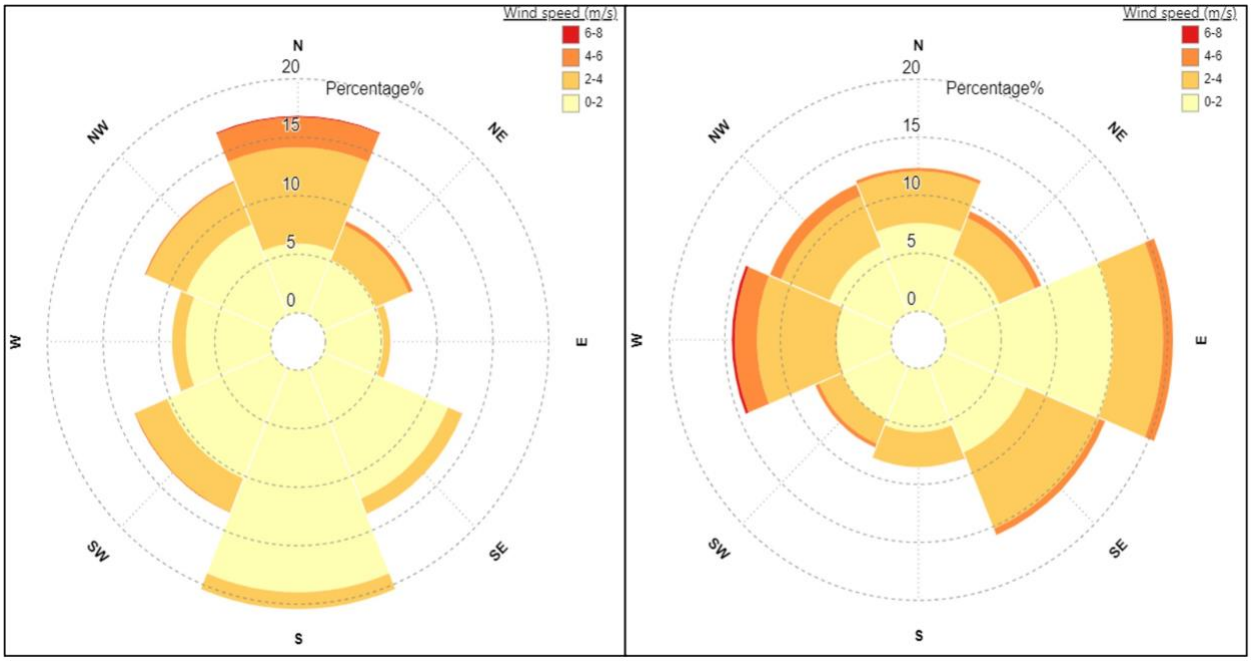


**Figure 16:**Wind speed and direction measurements made on the dock approximately 1 m above the lake surface (left) and on top of the east hummock in the uplands (right).

### 3.5 Discussion

The heat content of Lake Miwasin was calculated using the specific heat capacity of pure water (equation 6) introducing a known error as the water cap contains a mixture of fresh water and process effected water released from the tailings. As Lake Miwasin was constructed to be representative of future oil sands pit lakes, it has a low area to depth ratio compared to natural lakes. Gorham (1964) found that lakes with low area to depth ratios had increased capacity for heat storage, and that this effect was emphasized in small lakes. This feature likely manifested in Lake Miwasin as the maximum heat storage calculated for both study years was comparable with values calculated for both ponds (Touchart, 2016) and other small northern lakes (Rouse et al., 2005) despite the natural waterbodies being substantially larger in size and volume. Water clarity, thermocline depth, air temperature, and timing of ice cover loss are also known to influence lake

energy storage (Rouse et al., 2005; Nordbo et al., 2011), however their effects were not included in this study.

The timing of the maximum heat content is also a notable feature for lakes as it marks the transition between net energy sink to net energy source. In 2021, the maximum heat content of Lake Miwasin occurred on July 2nd, over a month earlier than 2020 (August 6th). Nordbo et al. (2011) also noted similar variations as the timing of the maximum heat content for a small northern lake in Finland oscillated between July and August over a four-year study period. Size affects timing of the maximum heat storage as small lakes in the Mackenzie River Valley reach their maximum heat content in July and early August, while large lakes reach their maximum heat content later in September (Oswald and Rouse, 2004; Rouse et al., 2005). Chang (2020) noted the maximum heat content for BML occurred on August 13 in 2015, which is representative of other medium size lakes as defined by Rouse et al. (2005). The collected data from both Lake Miwasin and BML suggest timing of the maximum heat content for oil sands pit lakes will be representative of natural northern lakes of similar size.

Lake size also influences surface energy fluxes as small lakes release energy earlier in the season as incoming radiation quickly warms the water causing strong temperature gradients between the lake surface and the lower atmosphere (Rouse et al., 2005; Wang et al., 2019). This is evident at Lake Miwasin as the sensible heat flux values were highest in May and June for both years, while the highest values at Base Mine Lake were measured in October (Clark et al., 2021). The latent heat flux at Lake Miwasin was also highest in June of both years, slightly preceding the maximum values measured at Base Mine Lake in August and September (Clark et al., 2021). When contrasting the atmospheric conditions with the variance of the latent and sensible heat flux values, stronger correlations are observed at Base Mine Lake for both surface fluxes (Clark et al., 2021).

This is in-part due to their size difference as surface wind speeds are lower for small lakes even if situated adjacent to large lakes is the same geographic setting (Wang et al., 2019). The surrounding landscape at Lake Miwasin may also be providing a sheltering effect reducing the wind speeds near the lake surface. As demonstrated in Figure 16, measurements on the top of the east hummock in the adjacent uplands indicate the dominant wind direction as east to west, where measurements made at the lake surface indicate south and north as the dominant directions. The low frequency of eastern and western winds at the lake surface are likely due to the presence of a forested edge ~ 20 m from the Lake Miwasin western shore and the elevated landscape features present in the adjacent uplands to the east. Similar sheltering effects have been observed to impact surface energy fluxes at a small pond in the Western Boreal Plains (Petrone et al., 2007) and a lake in the northern Canadian Shield (Spence et al., 2003).

The tailings thermal properties applied above were adopted from analysis completed on samples collected from BML (Dompierre and Barbour, 2017), which vary from the Lake Miwasin tailings as they did not undergo coagulant and flocculant addition prior to deposition. The thermal properties of the Lake Miwasin tailings are also likely to change with time as further consolidation occurs and sediment from the upland watershed continues to be introduced and deposited. Complimentary to the tailing's thermal properties, the sediment heat flux is influenced by the water temperature directly above the interface (Ragotzkie, 1978). The warm water temperatures in 2021 resulted in a net downward flux each month and higher energy migration into the tailings compared to 2020, when the tailings were supplying energy to the water column during May and early June. Despite the unique composition of oil sands tailings, the tailings heat flux values calculated for Lake Miwasin are comparable to values measured at similar depths in a small bog lake with soft sediments by Likens and Johnson, (1969).

As all the energy budget parameters were directly measured at Lake Miwasin, an open energy budget was completed with residual values included each month as a measure of error. Residual values were highest in the months that coincided with the largest changes in energy stored within the water column (May and October), followed by the months where the maximum heat content was achieved in each year (August 2020 and July 2021). One potential explanation for this is that the lake layers were assumed to be horizontally uniform in temperature and measured with a single temperature thermistor located in the approximate center. This resulted in large fluctuations in energy storage calculated from small and potentially local temperature changes measured at the sensor location. Another source of error occurred during 2021 as the lake stage decreased by ~ 30 cm and retreated beyond detection of the net radiometer mounted on the dock on the eastern shore. The net radiometer was relocated to an instrument pole located in the center of the lake, however there was a period of data lost as a result. The monitoring equipment was also removed from the lake in the middle of October providing data only from the first half of the month for both study seasons.

### 3.6 Conclusion

An open energy budget was completed for Lake Miwasin to quantify the energetics of the system and assess the influences brought about by the lakes physical characteristics. Despite being constructed at a pilot-scale, the timing and magnitude of the maximum heat content are comparable to small natural waterbodies. Wind action was reduced at the lake surface due to the small fetch and topography of the surrounding landscape contributing to lower correlations between climatic variables and the latent and sensible heat fluxes compared to the neighboring BML. The deposited tailings acted primarily as a heat sink during the open water season and the magnitude of the flux was responsive to elevated water temperatures. Energy budget closure was poorest during months

with the largest change in energy stored within the water column. Increased net radiation and temperatures in 2021 resulted in greater amounts of energy stored within the water column, higher levels of latent heat, and lower sensible heat compared to the wetter and slightly cooler 2020 season. This research indicates lake size, surrounding landscape features, and climatic conditions will all influence the energetics of future oil sands pit lakes constructed in the AOSR.

# Chapter 4 – Conclusion

While exploration of the AOSR has contributed to provincial and federal economic prosperity over the past 50 years, substantial alterations of the natural landscape and the vast volume of fluid tailings produced has left an environmental situation requiring sophisticated management. Oil sands pit lakes present a potential reclamation strategy by filling in large mined-out voids and sequestering FT through the water-capping treatment technology; however, research is still ongoing to prove their long-term viability. Provincial regulations require reclamation of FT through implementation of an approved technology that contributes to sustainable landscapes representative of a resilient and functional Boreal ecosystem (Government of Alberta, 2015; Alberta Energy Regulator, 2017). Sustainability of surface water features throughout the Boreal Plains ecozone is dependent on hydrologic connectivity with the surrounding landscape (Devito et al., 2012) as has been observed in both shallow lakes (Smerdon et al., 2005) and wetland-pond complexes (Petrone et al., 2007). As Lake Miwasin is currently the only oil sands pit lake constructed with an adjacent upland watershed and an un-controlled water balance, research on the lakes current design features is critical for evaluating the functionality and sustainability of future oil sands pit lakes throughout the AOSR.

Connectivity between Lake Miwasin and an existing groundwater table was considered negligible due to the presence of the clay liner, the sealing properties of the consolidated tailings, and the position of the lake basin being situated 10 m above the local aquifer. Research into the development of a shallow groundwater network within the constructed upland watershed is ongoing, however no data has been published to date. Freshwater additions to the lake during the open-water season were dependent on precipitation as sufficient rainfall triggered intermittent run-off events. These inflows sustained the lake volume and diluted the water cap above the

thermocline during periods of stratification. In dry periods with low rainfall, freshwater inputs to the lake were negligible and insufficient to off-set the loss from evaporation. As a result, dilution of the water-cap was inhibited contributing to an increased residence time. This research highlights the dependence of Lake Miwasin on adequate precipitation during the open water season to maintain a consistent water-cap in the absence of connectivity to a legacy groundwater system.

Although Lake Miwasin was constructed at a pilot-scale, the low surface area to depth ratio of the lake basin enabled energy absorption and storage values comparable with small natural northern lakes. The stored tailings beneath the water-cap acted as a heat sink during most of the open water season with rates responsive to water temperatures. The small fetch and sheltering effects of the surrounding landscape reduced wind action at the lake surface contributing to low correlations between climatic variables and the surface energy fluxes. Values for both latent and sensible heat fluxes measured at Lake Miwasin are expected to be lower than commercial-scale oil sands pit lakes due to decreased wind action at the lake surface and an earlier onset of the maximum heat content initiating the transition from energy sink to source. Overall, Lake Miwasin performed energetically like a typical northern lake by absorbing and storing high amounts of energy in the spring and early summer prior to releasing energy to the surrounding landscape in the fall.

Commissioned pit lakes in the AOSR will both influence and be influenced by the future climate of the Boreal Plains. The Boreal Plains climate is considered dry and generally water deficient with surplus moisture provided in cycles and stored within the subterrestrial glacial deposits (Devito et al., 2012). If the future climate of the Boreal Plains stays consistent, replenishment of this groundwater reservoir will be vital for the sustainability of constructed surface water bodies assuming hydrologic connectivity is established. Future climate estimates using general circulation models predict that the Boreal regions will become warmer, with less certainty applied to estimates

of water availability (Price et al., 2013; Wang et al., 2014). Although annual average precipitation is estimated to increase, inter-annual variability is also expected to increase and elevated temperatures will likely lead to higher rates of evapotranspiration potentially resulting in overall drier conditions (Price et al., 2013; Wang et al., 2014). Further modelling agreed with increased evapotranspiration rates but predicts wetter hydrologic and atmospheric conditions contributing to increased groundwater levels by the end of the century (Aquanty Inc., 2020). With uncertainty still expressed in future climate predictions, this data presented from Lake Miwasin provides valuable insight for the construction of robust and sustainable oil sands pit lakes in the AOSR.

# References


Alberta Energy Regulator, 2020. State of fluid tailings management for mineable oil sands, 2020. Retrieved from: https://static.aer.ca/prd/documents/reports/2020-State-Fluid-Tailings-Management-Mineable- OilSands.pdf.

Alberta Energy Regulator, 2017. Directive 085: Fluid tailings management for oil sands mining projects. Retrieved from: https://static.aer.ca/prd/documents/directives/Directive 085.pdf.

Ambrosetti, W., Barbanti, L., Sala, N., 2003. Residence time and physical processes in lakes. Journal of Limnology 62, 1–15.

Aquanty Inc., 2020. Impact of climate change on surface water and groundwater resources in the Athabasca river basin final project report.

Arriaga, D., Nelson, T.C., Risacher, F.F., Morris, P.K., Goad, C., Slater, G.F., Warren, L.A., 2019. The co-importance of physical mixing and biogeochemical consumption in controlling water cap oxygen levels in Base Mine Lake. Applied Geochemistry 111, 104442. https://doi.org/10.1016/j.apgeochem.2019.104442.

Aubinet, M., Vesala, T., Papale, D., 2012. Eddy Covariance: a practical guide to measurement and data analysis. Springer Netherlands, Dordrecht. https://doi.org/10.1007/978-94-007-2351-1.

Bell, R., 1884. Report on part of the Athabasca river, northwest territory, geological and natural history survey of Canada. Published by Authority of Parliament.

Bennett, K.E., Gibson, J.J., McEachern, P.M., 2008. Water-yield estimates for critical loadings assessment: Comparisons of gauging methods versus an isotopic approach. Canadian Journal of Fisheries and Aquatic Sciences 65, 83–99. https://doi.org/10.1139/F07-155.

Betts, A, K., Bartlo, J., 1991. The density temperature and the dry and wet adiabats. American Meteorological Society 119, 169–175.

BGC Engineering Inc., 2018a. Suncor Energy Inc. Demonstration pit lake tailings deposit, groundwater, and seepage monitoring instrumentation record.

BGC Engineering Inc., 2018b. Suncor Energy Inc. Demonstration pit lake hydrogeological instrumentation program.

Bowman, D.T., Warren, L.A., Slater, G.F., 2020. Isomer-specific monitoring of naphthenic acids at an oil sands pit lake by comprehensive two-dimensional gas chromatography–mass spectrometry. Science of the Total Environment 746, 140985. https://doi.org/10.1016/j. scitotenv.2020.140985.

Brinker, C., Symbaluk, M., Boorman, R. L., 2011. Constructing habitat for a sustainable native fisheries in the Sphinx Lake end pit lake system, in: Proceedings of the Sixth International Conference on Mine Closure. Australian Centre for Geomechanics, Perth, pp. 525–534. https://doi.org/10.36487/acg_rep/1152_55_brinker.

Brown, G.W., 1969. Predicting temperatures of small streams. Water Resources Research 5(1), 68–75. https://doi.org/10.1029/WR005i001p00068.

Burba, G., 2013. Eddy covariance method for scientific, industrial, agricultural, and regulatory applications. LI-COR Biosciences.

Burkus, Z., Wheler, J., Pletcher, S., Wheler, J., Pletcher, S., 2014. GHG emissions from oil sands tailings ponds: Overview and modelling based on fermentable substrates. Alberta Environment and Sustainable Resource Development.

Canada's Oil Sands Innovation Alliance (COSIA), 2021. Pit Lakes: A surface mining perspective, Tailings Environmental Priority Area (EPA).

Canadian Association of Petroleum Producers (CAPP), 2022. Canada's oil sands fact book. Retrieved from: https://www.capp.ca/publications/canadas-oil-sands-fact-book/.

Castendyk, D., Charette, T., Hrynyshyn, J., Kupper, A., McKenna, G., Mooder, B., Sellick, A., Shuttleworth, D., Vandenberg, J., Wylynko, D., 2012. End pit lakes guidance document. Fort McMurray, AB.

Castro, J.M., Moore, J.N., 2000. Pit lakes: their characteristics and potential for remediation. Environmental Geology 39, 1254–1260. https://doi.org/https://doi.org/10.1007/s002549 900100.

Chang, S., 2020. Heat budget for an oil sands pit lake. University of British Columbia.

Chastko, P., 2004. Developing alberta's oil sands. University of Calgary Press.

Clark, M.G., Drewitt, G.B., Carey, S.K., 2021. Energy and carbon fluxes from an oil sands pit lake. Science of the Total Environment 752, 141966. https://doi.org/10.1016/j.scitotenv. 2020.141966.

Cole, J.J., Pace, M.L., 1998. Hydrologic Variability of small, northern Michigan lakes measured by the addition of tracers. Ecosystems 1, 310–320. https://doi.org/10.1007 /s100219900024.

Cole, T.M., Wells, S.A., 2003. "CE-QUAL-W2: A two-dimensional, laterally averaged, hydrodynamic and water quality model, Version 3.1," Instruction Report EL-03-1, US Army Engineering and Research Development Center, Vicksburg, MS.

Davies-Colley, R.J., 1988. Mixing depths in New Zealand lakes. New Zealand Journal of Marine and Freshwater Research 22(4), 517–528. https://doi.org/10.1080/00288330.1988.9516322.

Devito, K., Creed, I., Gan, T., Mendoza, C., Petrone, R., Silins, U., Smerdon, B., 2005. A framework for broad-scale classification of hydrologic response units on the Boreal Plain: Is topography the last thing to consider? Hydrological Processes 19, 1705–1714. https://doi.org/10.1002/hyp.5881.

Devito, K., Mendoza, C., Qualizza, C., 2012. Conceptualizing water movement in the Boreal Plains. Implications for watershed reconstruction. https://doi.org/10.7939/R32J4H.

Devito, K.J., Hokanson, K.J., Moore, P.A., Kettridge, N., Anderson, A.E., Chasmer, L., Hopkinson, C., Lukenbach, M.C., Mendoza, C.A., Morissette, J., Peters, D.L., Petrone, R.M., Silins, U., Smerdon, B., Waddington, J.M., 2017. Landscape controls on long-term runoff in subhumid heterogeneous Boreal Plains catchments. Hydrological Processes 31, 2737–2751. https://doi.org/10.1002/hyp.11213.

Dompierre, K.A., Barbour, S.L., 2017. Thermal properties of oil sands fluid fine tailings: laboratory and in situ testing methods. Canadian Geotechnical Journal 54, 428–440. https://doi.org/10.1139/cgj-2016-0235.

Dompierre, K.A., Lindsay, M.B.J., Cruz-Hernández, P., Halferdahl, G.M., 2016. Initial geochemical characteristics of fluid fine tailings in an oil sands end pit lake. Science of the Total Environment 556, 196–206. https://doi.org/10.1016/j.scitotenv.2016.03.002.

Eary, L.E., 1998. Predicting the effects of evapoconcentration on water quality in mine pit lakes. Journal of Geochemical Exploration 64, 223–236. https://doi.org/https://doi.org/10.1016 /S0375-6742(98) 00035-1.

Eger, C.G., Chandler, D.G., Roodsari, B.K., Davidson, C.I., Driscoll, C.T., 2014. Water budget triangle: A new conceptual framework for comparison of green and gray infrastructure, in: ICSI 2014: Creating Infrastructure for a Sustainable World - Proceedings of the 2014 International Conference on Sustainable Infrastructure. American Society of Civil Engineers (ASCE), pp. 1010–1017. https://doi.org/10.1061/9780784478745.095.

Elsawwaf, M., Willems, P., 2012. Analysis of the climate variability on Lake Nasser evaporation based on the bowen ratio energy budget method. Journal of Environmental Biology 33, 475–485.

Fair, A., 2014. Oil sands tailings: an historical perspective, in: Sego, D., Wilson, G.W., Beier, N. (Eds.), Proceedings of the Fourth International Oil Sands Tailings Conference. University of Alberta, Department of Civil and Environmental Engineering, Lake Louise.

Fang, X., Stefan, H.G., 1996. Dynamics of heat exchange between sediment and water in a lake. Water Resources 32, 1719–1727.

Fenton, M.M., Schreiner, B.T., Nielsen, E., Pawlowicz, J.G., 1994. Quaternary geology of the western plains, in: Mossip, G.D., Shesten, I. (Eds.), Atlas of the Western Canada Sedimentary Basin. Canadian Society of Petroleum Geologists and Alberta Research Council.

Ferone, J.M., Devito, K.J., 2004. Shallow groundwater-surface water interactions in pond-peatland complexes along a Boreal Plains topographic gradient. J Hydrology 292, 75–95. https://doi.org/10.1016/j.jhydrol.2003.12.032.

Fiedler, P.C., 2010. Comparison of objective descriptions of the thermocline. Limnology and Oceanography: Methods 8, 313–325. https://doi.org/10.4319/lom.2010.8.313.

Fischer, H.B., List, E.J., Koh, R., Imberger, J., Brooks, N.H., 1979. Mixing in inland and coastal waters. Academic Press, London.

Foken, T., Leclerc, M.Y., 2004. Methods and limitations in validation of footprint models. Agricultural and Forest Meteorology 127, 223–234. https://doi.org/10.1016/j.agrformet .2004.07.015.

Forel, F. A., 1880. Temperatures lacustres: recherches sur la temperature du lac Leman et d'autres lacs d'eau douce. Deuxieme serie. Archives des sciences physiques et naturelles 3, 89–106.

Gammons, C.H., Tech, M., Harris, L.N., Castro, J.M., Cott, P.A., Hanna, B.W., 2009. Creating lakes from open pit mines: processes and considerations, emphasis on northern environments. Canadian Technical Report of Fisheries and Aquatic Sciences 2826, 1–116.

Gianniou, S.K., Antonopoulos, V.Z., 2007. Evaporation and energy budget in Lake Vegoritis, Greece. Journal of Hydrology 345, 212–223. https://doi.org/10.1016/j.jhydrol.2007.08.007.

Gibson, J.J., 2002. Short-term evaporation and water budget comparisons in shallow Arctic lakes using non-steady isotope mass balance. Journal of Hydrology 264, 242–261. https://doi.org /10.1016/S0022-1694(02)00091-4.

Gibson, J.J., Birks, S.J., Yi, Y., Vitt, D.H., 2015. Runoff to boreal lakes linked to land cover, watershed morphology and permafrost thaw: A 9-year isotope mass balance assessment. Hydrological Processes 29, 3848–3861. https://doi.org/10.1002/hyp.10502.

Gibson, J.J., Prepas, E.E., Mceachern, P., 2002. Quantitative comparison of lake throughflow, residency, and catchment runoff using stable isotopes: modelling and results from a regional survey of Boreal lakes. Journal of Hydrology 262, 128–144. https://doi.org/10.1016/S0022-1694(02)00022-7.

Golder Associates, 2017. Literature review of global pit lakes: pit lake-case studies.

Gorham, E., 1964. Morphometric control of annual heat budgets in temperate lakes. Limnology and Oceanography 9, 525–529. https://doi.org/https://doi.org/10.4319/lo.1964.9.4.0525.

Gosselin, P., Hrudey, S., Naeth, M.A., Plourde, A., Therrien, R., Van Der Kraak, G., Xu, Z., 2010. Environmental and health impacts of Canada's oil sands industry. Royal Society of Canada.

Government of Alberta, 2023. Environmental protection and enhancement act, Alberta Queen's Printer. Retrieved from: https://kings-printer.alberta.ca/570.cfm?frm_isbn=9780779841660 &search_by=link.

Government of Alberta, 2020. Oil sands tenure regulation. Retrieved from: https://kings-printer.alberta.ca/570.cfm?frm_isbn=9780779817627&search_by=link.

Government of Alberta, 2015. Tailings management framework for mineable athabasca oil sands (TMF). Retrieved from: https://open.alberta.ca/dataset/962bc8f4-3924-46ce-baf8-d6b7a26467ae/resource/7c49eb63-751b-49fd-b746-87d5edee3131/download/2015-larp-tailingsmgtathabascaoilsands.pdf.

Government of Alberta, 2012. Lower Athabasca regional plan. Retrieved from: https://open. alberta.ca/dataset/37eab675-19fe-43fd-afff-001e2c0be67f/resource/a063e2df-f5a6-4bbd-978c-165cc25148a2/download/5866779-2012-08-lower-athabasca-regional-plan-2012-2022.pdf.

Government of Canada, 2023. Canadian climate normals 1981-2012 station data. https://climate. weather.gc.ca/climate_normals/results_1981_2010_e.html?stnID=2519&autofwd=1 (accessed 12.17.23).

Grimaldi, R., 2009. Climatological characteristics, in: Castendyk, D.N., Eary, L.E. (Eds.), Mine pit lakes: Characteristics, predictive modeling and sustainability. Society for Mining, Metallurgy and Exploration.

Hatfield, 2022. Lake Miwasin Physical Limnology Annual Report.

Healy, R.W., Winter, T.C., LaBaugh, J.W., Franke, O.L., 2007. Water budgets: Foundations for effective water-resources and environmental management. US Geological Survey Circular 1308.

Humphries, M., 2007. North American oil sands: History of development, prospects for the future, Congressional Research Service.

Imboden, D.M., Wuest, A., 1995. Mixing mechanisms in lakes, in: Physics and Chemistry of Lakes. Springer, Berlin, Heidelberg, pp. 83–138.

Ireson, A.M., Barr, A.G., Johnstone, J.F., Mamet, S.D., van der Kamp, G., Whitfield, C.J., Michel, N.L., North, R.L., Westbrook, C.J., DeBeer, C., Chun, K.P., Nazemi, A., Sagin, J., 2015. The changing water cycle: the Boreal Plains ecozone of Western Canada. Wiley Interdisciplinary Reviews: Water 2.5, 505–521. https://doi.org/10.1002/wat2.1098.

Kabwe, L.K., Scott, J.D., Beier, N.A., Wilson, G.W., Jeeravipoolvarn, S., 2019. Environmental implications of end pit lakes at oil sand mines in Alberta, Canada. Environmental Geotechnics 6, 67–74. https://doi.org/10.1680/jenge.17.00110.

Kaimal, J.C., Finnigan, J.J., 1994. Atmospheric boundary layer flows. Oxford University Press. https://doi.org/10.1093/oso/9780195062397.001.0001.

Ketcheson, S.J., Price, J.S., 2016. A comparison of the hydrological role of two reclaimed slopes of different age in the Athabasca oil sands region, Alberta, Canada. Canadian Geotechnical Journal 53, 1553–1546. https://doi.org/https://doi.org/10.1139/cgj-2015-0391.

Ketcheson, Scott J., Price, J.S., 2016. Snow hydrology of a constructed watershed in the Athabasca oil sands region, Alberta, Canada. Hydrological Processes 30, 2546–2561. https://doi. org/10.1002/hyp.10813.

Kljun, N., Calanca, P., Rotach, M.W., Schmid, H.P., 2015. A simple two-dimensional parameterisation for flux footprint prediction (FFP). Geoscientific Model Development 8, 3695–3713. https://doi.org/10.5194/gmd-8-3695-2015.

Lenters, J.D., Kratz, T.K., Bowser, C.J., 2005. Effects of climate variability on lake evaporation: Results from a long-term energy budget study of Sparkling Lake, northern Wisconsin (USA). Journal of Hydrology308, 168–195. https://doi.org/10.1016/j.jhydrol.2004.10.028.

Levenspiel, O., 1998. Chemical reaction engineering, 3rd ed. John Wiley & Sons.

Likens, G.E., Johnson, N.M., 1969. Measurement and analysis of the annual heat budget for the sediments in two Wisconsin lakes. Limnology and Oceanography 14, 115–135. https://doi.org /10.4319/lo.1969.14.1.0115.

Lund, M., van Etten, E., Polifka, J., Vasquez, M.Q., Ramessur, R., Yangzom, D., Blanchette, M.L., 2020. The importance of catchments to mine-pit lakes: Implications for closure. Mine Water and Environment 39, 572–588. https://doi.org/10.1007/s10230-020-00704-8.

Mccullough, C., Marchant, G., Unseld, J., Robinson, M., O'grady, B., 2012. Pit lakes as evaporative "terminal" sinks: an approach to best available practice mine closure., in: Proceedings of the International Mine Water Association Symposium. Bunbury, Australia, pp. 167–174.

Mccullough, C., Radhakrishnan, N., Lund, M., Newport, M., Ballot, E., Short, D., 2012. Riverine breach and subsequent decant of an acidic pit lake: evaluating the effects of riverine flow-through on lake stratification and chemistry, in: Proceedings of the International Mine Waters Conference. International Mine Water Association, Bunbury, Australia, pp. 533–540.

McCullough, C.D., Marchand, G., Unseld, J., 2013. Mine closure of pit lakes as terminal sinks: best available practice when options are limited? Mine Water and Environment 32, 302–313. https://doi.org/10.1007/s10230-013-0235-7.

McCullough, C.D., Schultze, M., 2018. Engineered river flow-through to improve mine pit lake and river values. Science of the Total Environment 640–641, 217–231. https://doi.org/ 10.1016/j.scitotenv.2018.05.279.

Monsen, N.E., Cloern, J.E., Lucas, L.V., Monismith, S.G., 2002. A comment on the use of flushing time, residence time, and age as transport time scales. Limnology and Oceanography 475, 1545–1553. https://doi.org/https://doi.org/10.4319/lo.2002.47.5.1545.

Nordbo, A., Launiainen, S., Mammarella, I., Leppäranta, M., Huotari, J., Ojala, A., Vesala, T., 2011. Long-term energy flux measurements and energy balance over a small boreal lake using eddy covariance technique. Journal of Geophysical Research: Atmospheres 116, 1–17. https://doi.org/10.1029/2010JD014542.

Oswald, C.J., Rouse, W.R., 2004. Thermal characteristics and energy balance of various-size Canadian Shield lakes in the Mackenzie River basin. Journal of Hydrometeorology 5, 129–144. https://doi.org/10.1175/1525-7541(2004)005<0129:TCAEBO>2.0.CO;2.

Petermann, E., Gibson, J.J., Knöller, K., Pannier, T., Weiß, H., Schubert, M., 2018. Determination of groundwater discharge rates and water residence time of groundwater-fed lakes by stable isotopes of water (18O, 2H) and radon (222Rn) mass balances. Hydrological Processes 32, 805–816. https://doi.org/10.1002/hyp.11456.

Petrone, R.M., Silins, U., Devito, K.J., 2007. Dynamics of evapotranspiration from a riparian pond complex in the western Boreal Forest, Alberta, Canada. Hydrological Processes 21, 1391–1401. https://doi.org/10.1002/hyp.6298.

Pieters, R., Lawrence, G.A., 2014. Physical processes and meromixis in pit lakes subject to ice cover. Canadian Journal of Civil Engineering 41, 569–578. https://doi.org/10.1139/cjce-2012-0132.

Pilotti, M., Simoncelli, S., Valerio, G., 2014a. A simple approach to the evaluation of the actual water renewal time of natural stratified lakes. Water Resources Research 50, 2830–2849. https://doi.org/10.1002/2013WR014471.

Pilotti, M., Simoncelli, S., Valerio, G., 2014b. Computing the transport time scales of a stratified lake on the basis of Tonolli's model. Journal of Limnology 73. https://doi.org/10.4081/ jlimnol.2014.897.

Piontelli, R., Tonolli, V., 1964. Il tempo di residenza delle acque lacustri in relazione ai fenomeni di arricchimento in sostanze immesse, con particolare riguardo al Lago Maggiore. Mem. Ist. Ital. Idrobiol 17, 247–266.

Poon, H.Y., Brandon, J.T., Yu, X., Ulrich, A.C., 2018. Turbidity mitigation in an oil sands pit lake through pH reduction and freshwater addition. Journal of Environmental Engineering 144, 1–7. https://doi.org/10.1061/(ASCE)EE.1943-7870.0001472.

Price, D.T., Alfaro, R.I., Brown, K.J., Flannigan, M.D., Fleming, R.A., Hogg, E.H., Girardin, M.P., Lakusta, T., Johnston, M., McKenney, D.W., Pedlar, J.H., Stratton, T., Sturrock, R.N., Thompson, I.D., Trofymow, J.A., Venier, L.A., 2013. Anticipating the consequences of climate change for Canada's boreal forest ecosystems. Environmental Reviews 21, 322–365. https://doi.org/10.1139/er-2013-0042.

Quinn, F.H., 1992. Hydraulic residence time for the laurenitian great lakes. Journal of Great Lakes Research 22–28. https://doi.org/https://doi.org/10.1016/S0380-1330(92)71271-4.

R Core Team, 2021. R: a language and environment for statistical computing. R Foundation for Statistical Computing, Vienna, Austria. https://www.R-project.org/.

Ragotzkie, R.A., 1978. Heat Budgets of Lakes, in: Lakes. pp. 1–19. https://doi.org/10.1007/978-1-4757-1152-3_1.

Read, J.S., Hamilton, D.P., Jones, I.D., Muraoka, K., Winslow, L.A., Kroiss, R., Wu, C.H., Gaiser, E., 2011. Derivation of lake mixing and stratification indices from high-resolution lake buoy data. Environmental Modelling and Software 26, 1325–1336. https://doi.org/ 10.1016/j.envsoft.2011.05.006.

Read, P., 2014. Broad suite of practice and technology key to success in tailings mangement, in: Sego, D., Wilson, G.W., Beier, N. (Eds.), Proceedings of the Fourth International Oil Sands Tailings Conference. University of Alberta Department of Civil & Environmental Engineering, Lake Louise.

Reichstein, M., Falge, E., Baldocchi, D., Papale, D., Aubinet, M., Berbigier, P., Bernhofer, C., Buchmann, N., Gilmanov, T., Granier, A., Grunwald, T., Havrankova, K., Ilvesniemi, H., Janous, D., Knohl, A., Laurila, T., Lohila, A., Loustau, D., Matteucci, G., Meyers, T., Miglietta, F., Ourcival, J.-M., Pumpanen, J., Rambal, S., Rotenberg, E., Sanz, M., Tenhunen, J., Seufert, G., Vaccari, F., Vesala, T., Yakir, D., Valentini, R., 2005. On the separation of net ecosystem exchange into assimilation and ecosystem respiration: review and improved algorithm. Global Change Biology 11, 1424–1439. https://doi.org/10.1111/j. 1365-2486.2005.001002.x.

Risacher, F.F., Morris, P.K., Arriaga, D., Goad, C., Nelson, T.C., Slater, G.F., Warren, L.A., 2018. The interplay of methane and ammonia as key oxygen consuming constituents in early stage development of Base Mine Lake, the first demonstration oil sands pit lake. Applied Geochemistry 93, 49–59. https://doi.org/10.1016/j.apgeochem.2018.03.013.

Rosenberry, D.O., Sturrock, A.M., Winter, T.C., 1993. Evaluation of the energy budget method of determining evaporation at Williams Lake, Minnesota, using alternative instrumentation and study approaches. Water Resource Research 29, 2473–2483.

Rouse, W.R., Oswald, C.J., Binyamin, J., Spence, C., Schertzer, W.M., Blanken, P.D., Bussières, N., Duguay, C.R., 2005. The role of northern lakes in a regional energy balance. Journal of Hydrometeorology 6, 291–305. https://doi.org/10.1175/JHM421.1.

Rueda, F.J., Cowen, E.A., 2005. Residence time of a freshwater embayment connected to a large lake. Limnology and Oceanography 50, 1638–1653. https://doi.org/https://doi.org/10. 4319/lo.2005.50.5.1638.

Schmidt, A., Gibson, J.J., Santos, I.R., Schubert, M., Tattrie, K., Weiss, H., 2010. The contribution of groundwater discharge to the overall water budget of two typical boreal lakes in Alberta/Canada estimated from a radon mass balance. Hydrology and Earth Science Systems 14, 79–89. https://doi.org/https://doi.org/10.5194/hess-14-79-2010.

Schramm, L.L., Stasiuk, E. N., Turner, D., 2001. The influence of interfacial tension in the hot- water process for recovering bitumen from the Athabasca oil sands. Canadian International Petroleum Conference.

Smerdon, B.D., Devito, K.J., Mendoza, C.A., 2005. Interaction of groundwater and shallow lakes on outwash sediments in the sub-humid Boreal Plains of Canada. Journal of Hydrology 314, 246–262. https://doi.org/10.1016/j.jhydrol.2005.04.001.

Spence, C., Rouse, W.R., Worth, D., Oswald, C., 2003. Energy budget processes of a small northern lake. Journal of Hydrometeorology 4, 694–701. https://doi.org/10.1175/1525-7541(2003)004<0694:EBPOAS>2.0.CO;2.

Spigel, R.H., Imberger, J., 1980. The classification of mixed-layer dynamics of lakes of small to medium size. Journal of Physical Oceanography 10, 1104–1120. https://doi.org/10.1175/ 1520-0485(1980)010%3C1104:TCOMLD%3E2.0.CO;2.

Sturrock, A.M., Winter, T.C., Rosenberry, D.O., 1992. Energy budget evaporation from Williams Lake: a closed lake in north central Minnesota. Water Resources 28, 1605–1617.

Tedford, E., Halferdahl, G., Pieters, R., Lawrence, G.A., 2019. Temporal variations in turbidity in an oil sands pit lake. Environmental Fluid Mechanics 19, 457–473. https://doi.org/10. 1007/s10652-018-9632-6.

Thomson, R.E., Fine, I. V., 2003. Estimating mixed layer depth from oceanic profile data. Journal of Atmospheric and Oceanic Technology 20, 319–329. /https://doi.org/10.1175/ 1520-0426(2003)020%3C0319:EMLDFO%3E2.0.CO;2.

Touchart, L., 2016. Heat budget of ponds: Epistemological examination and application to ponds in Limousin. Annales de Geographie, 143–169. https://doi.org/10.3917/ag.708.0143.

Touchart, L., Bartout, P., 2012. Thermoclines in ponds: a new typology by the study of continuous water temperature measurements. International Conference Water Resources and Wetlands, Romania Limnogeographical Association. 27-32. hal-02096795.

Vallentyne, J.R., 1957. Principles of modern limnology. American Scientist 45, 218–244.

Walker, D.J., 1998. Modelling residence time in stormwater ponds. Ecological Engineering 10, 247–262. https://doi.org/https://doi.org/10.1016/S0925-8574(98)00016-0.

Wang, B., Ma, Y., Wang, Y., Su, Z., Ma, W., 2019. Significant differences exist in lake-atmosphere interactions and the evaporation rates of high-elevation small and large lakes. Journal of Hydrology 573, 220–234. https://doi.org/10.1016/j.jhydrol.2019.03.066.

Wang, Y., Hogg, E.H., Price, D.T., Edwards, J., Williamson, T., 2014. Past and projected future changes in moisture conditions in the Canadian boreal forest. The Forestry Chronicle 90, 678–691. https://doi.org/10.5558/tfc2014-134.

Webb, E.K., Pearman, G.I., Leuning, R., 1980. Correction of flux measurements for density effects due to heat and water vapour transfer. Quarterly Journal of the Royal Meteorological Society 106, 85–100. https://doi.org/10.1002/qj.49710644707.

Wetzel, R., 2001. Limnology: lake and river ecosystems 3rd edition. Elsevier Academic Press.

White, K.B., Liber, K., 2020. Chronic toxicity of surface water from a Canadian oil sands end pit lake to the freshwater invertebrates Chironomus dilutus and Ceriodaphnia dubia. Archives of Environmental Contamination and Toxicology 78, 439–450. https://doi.org/10.1007 /s00244-020-00720-3.

Winter, T.C., Buso, D.C., Rosenberry, D.O., Likens, G.E., Sturrock, A.M., Mau, D.P., 2003. Evaporation determined by the energy-budget method for Mirror Lake, New Hampshire. Limnology and Oceanography 48, 995–1009. https://doi.org/10.4319/lo.2003.48.3.0995.

Xenopoulos, M.A., Schindler, D.W., 2001. The environmental control of near-surface thermoclines in boreal lakes. Ecosystems 4, 699–707. https://doi.org/10.1007/s10021-001-0038-8.

Yu, X., Lee, K., Ulrich, A.C., 2019. Model naphthenic acids removal by microalgae and Base Mine Lake cap water microbial inoculum. Chemosphere 234, 796–805. https://doi.org /10.1016/j.chemosphere.2019.06.110.

Zabel, A., Ketcheson, S.J., Petrone, R.M., 2023. Climatic controls on the water balance of a pilot-scale oil sands mining pit lake in the Athabasca oil sands region, Canada. International Journal of Mining, Reclamation and Environment 38:4, 306-323. https://doi.org/10.1080 /17480930.2023.2270301.

Zhao, J., Zhang, M., Xiao, W., Wang, W., Zhang, Z., Yu, Z., Xiao, Q., Cao, Z., Xu, J., Zhang, X., Liu, S., Lee, X., 2019. An evaluation of the flux-gradient and the eddy covariance method to measure CH4, CO2, and H2O fluxes from small ponds. Agriculture and Forest Meteorology 275, 255–264. https://doi.org/10.1016/j.agrformet.2019.05.032.